1991

The application of a computer simulator to a generalized describing function method

Ibarra C. Jaculbe III
Lehigh University

THE APPLICATION OF A

COMPUTER SIMULATOR TO A GENERALIZED

DESCRIBING FUNCTION METHOD

by

Ibarra C. Jaculbe III.

A Thesis

Presented to the Graduate Committee

of Lehigh University

in Candidacy for the Degree of

Master of Science

in

Electrical Engineering

Lehigh University

1991

This thesis is accepted in partial fulfillment of the requirements for the degree of Master of Science.

MAY 8, 1991

(date)

Douglas Frey

Professor in Charge

Lawrence J. Vanecin

Department Chairman

Acknowledgements

I would like to thank the following people who made invaluable contributions in making this thesis possible:

To my adviser, Dr. Douglas R. Frey for introducing me to his original ideas for a generalized describing function method, and giving me the opportunity to work on it's development, for providing me insight and motivation throughout this research project, and carefully reviewing the text of this document.

To my family for their love and support. To my father Ibarra Jr., my mother Alpha, my sister Alphita, and Mamay and Niel.

To Shiela J. Hiceta for her encouragements and concern throughout my two years of study.

To the faculty and staff of the Computer Science and Electrical Engineering Department who were always there to provide help when I needed them.

And to the United States Agency for International Development through the Asia Foundation for funding my studies.

Table of Contents

List of Figures

List of Tables

Abstract

General purpose circuit simulators find the periodic steady-state solution of nonlinear networks using transient analysis. This method is computationally expensive for lightly damped circuits where the transients could last for hundreds of periods. To solve this problem, a frequency domain algorithm is introduced, coined as the *Generalized Describing Function Method* (GDF), which combines the simplicity of the classical describing function method and the accuracy of the harmonic balance method to carry out harmonic analysis. The capabilty to use the SPICE AC analysis as it's front end tool makes the GDF a prospective general nonlinear circuit simulator. The mathematical formulations are presented, the computational implementation discussed, and the performance of the algorithm is tested on polynomial nonlinearities. The algorithm shows exceptionally fast convergence on circuits with low harmonic distortion, but the convergence slows down when the harmonic distortion is enlarged. The use of a weighting function to operate on the error vector, however, improves convergence considerably.

Introduction

The mathematical complexity involved in the study of nonlinear networks has always intrigued engineers who venture into this field. Voluminous literature has been written on this subject, mostly exploring the theoretical issues, although recently practical applications have been touched as well. The notoriety of nonlinear networks to defy analytical schemes is well documented, and it is acknowledged that approximation using computational techniques has been the most desirable method of study. In fact, numerous textbooks have been written that deal with computer-aided design and simulation of nonlinear circuits.

Circuit simulators traditionally find the steady-state solution of networks using a time domain approach. However, this method experiences problems when it is used to study the steady-state behavior of even the most common of nonlinear circuits with a sinusoidal input and periodic response. In theory, the periodic response can be obtained by integrating the dynamic equations that describe the system until the transient components become negligible. These could take hundreds of periods in some situations-for example, in lightly damped sytems such as oscillators-and the simulation then becomes expensive. One widely discussed procedure to speed up the solution of lengthy transient conditions by approaching it as a two-point boundary value problem is called the "shooting method" [1], [2]; however, this is also based in the time

domain, and involves numerical integration of differential equations, and therefore is also computationally expensive. It is evident that a frequency domain based analysis is needed.

One of the first enthusiasts of the frequency domain solution was Kochenburger [3], who used a harmonic approach to synthesize nonlinear contactor servomechanisms. He named his scheme the "describing function" method, which is essentially approximating the output of the nonlinearity with only the fundamental frequency, and assumes that higher harmonics are effectively filtered out by the other components of the system. This method has become the standard analytical tool in the study of nonlinear feedback control systems, but is inaccurate in representing circuits whose signals have strong harmonic content, and, therefore, has never become popular in computer-aided simulations. Another popular frequency domain solution technique is the harmonic balance method, and is basically an extension of the describing function method, in that the nonlinearity is represented by a filter function so higher harmonics can be carried over in the solution. One of the earliest discussions on the harmonic balance method was by Nahkla and Vlach [4], and since then this method has appeared extensively in literature. The harmonic balance method has been applied as a numerical algorithm in various fields of nonlinear circuit study-for example, distortion analysis of nonlinear networks [5], and analysis of microwave class-C amplifiers [6], and Schottky-diode mixers [7]. However, because it has a relatively large number of variables to be optimized, the

harmonic balance method has never been implemented in general circuit simulators, which, up to this time, still use the time domain approach to solve nonlinear networks using variations of classical algorithms, like the Newton-Raphson and predictor-corrector methods.

The purpose of this thesis is to introduce a numerical algorithm which takes advantage of the simplicity of the describing function method and the ability of the harmonic balance method to do harmonic analysis, and to present examples of experiments that were conducted to test it's performance on different types and levels of nonlinearities. An overview of the describing function method is given in the first chapter. In chapter 2, the governing equations are derived from the harmonic balance point-of-view, which are then slightly modified to form the numerical algorithm presented here. In chapter 3, the role of the SPICE AC analysis, and other computational issues are discussed. Results of the experiments conducted are shown in chapter 4. These results can be classified into three groups: data gathered by using only the fundamental harmonic; those coming from the use of multiple harmonics on circuits with small harmonic distortion; and those coming from the use of multiple harmonics on circuits with large harmonic distortion. Finally, conclusions of the study are presented, together with an outline of future research directions.

Chapter 1
The Describing Function Method

The describing function method is used to perform an approximate analysis of a given nonlinear system. The linear operator which is used to closely match the transfer characteristics of a nonlinear element is called the *describing function*. Different forms of signals can be expected to appear at the input of the nonlinear element, and since the describing function is generally a function of that signal, we expect to have a specific describing function for each input signal form. We will use the classical feedback system with a nonlinear forward gain to introduce the basic concepts, and then we will discuss how the describing function is derived for one form of input signal, that of a sinusoid. For other forms of input signal, refer to the discussion by Gelb and Vander Velde [8].

1.1 The Principle

The feedback system shown in Figure 1.1a has a nonlinear element $N(e)$ as the forward gain, a linear element $G(.)$ in the feedback loop, and is subjected to an input signal u. The output signal is given as by

$$x = N(e) \tag{1.1}$$

The error signal is

$$e = u - Gx \tag{1.2}$$

Therefore:

$$x = N(u - Gx) \tag{1.3}$$

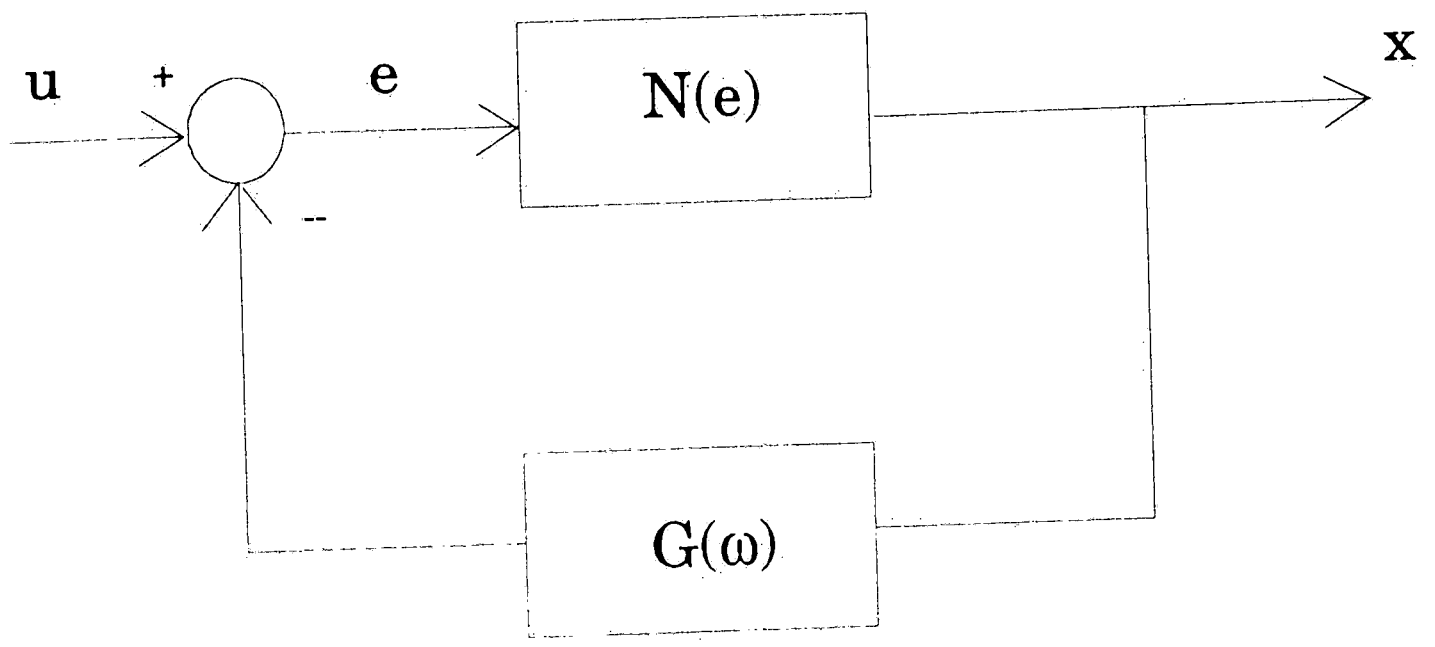

(a)

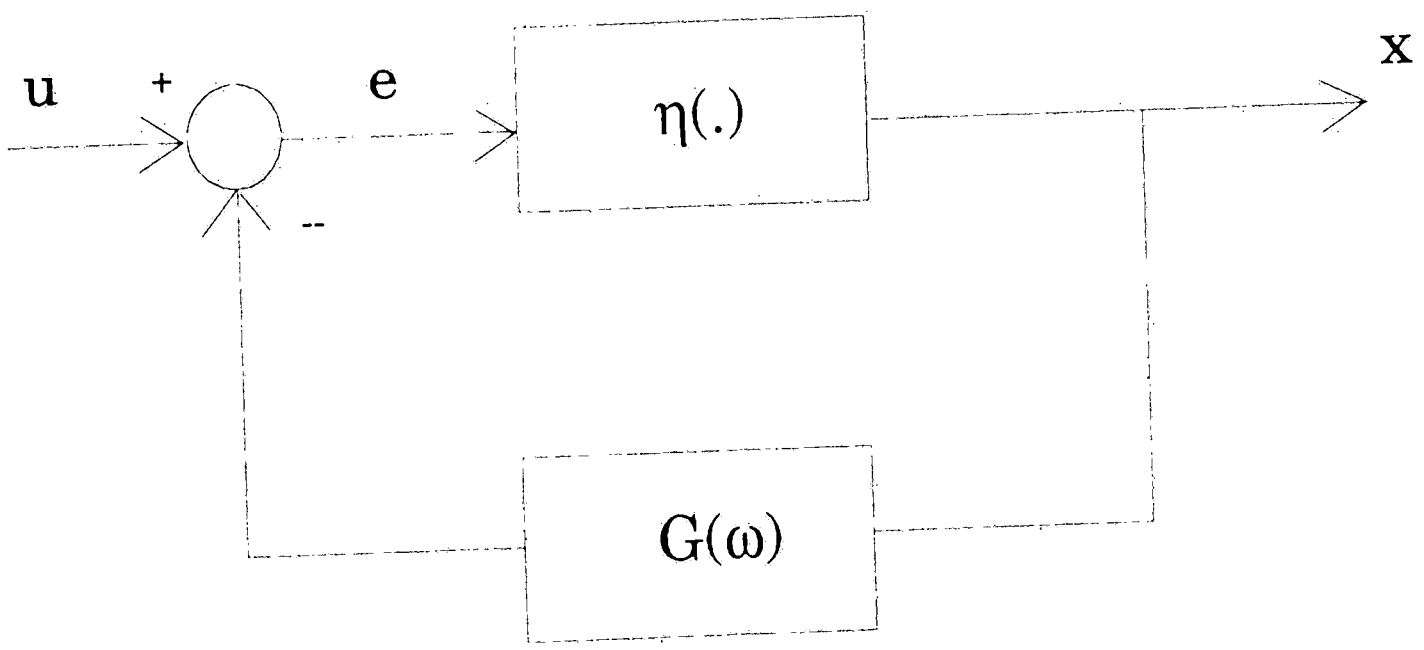

(b)

Figure 1-1: A feedback system with nonlinear gain.

Since (1.3) is a nonlinear equation, it's solution cannot not be expressed in closed form. Before carrying out further analysis, we approximate the nonlinearity as follows:

$$N(e) = \eta(.)e \tag{1.4}$$

Where $\eta(.)e$ is interpreted as the output of a linear time-invariant device with the input e and the transfer function $\eta(.)$. The linear operator $\eta(e)$ is the describing function. It is substituted into the system as shown in figure 1.1b. Combining (1.1) and (1.4) we have

$$x = \eta(.)e \tag{1.5}$$

and since $e = u - Gx$ we have

$$x = \frac{\eta(.)u}{1+\eta(.)G} \tag{1.6}$$

Note that (1.6) has the form of a general feedback equation with the forward gain being the operator $\eta(.)$. The basic idea here would be to find the optimum value of the operator $\eta(.)$ so as to make the linear system aproximate it's nonlinear equivalent under the given circumstances.

1.2 Sinusoidal Input to the Nonlinearity

The most popular application for the describing function method is the prediction of limit cycles of nonlinear feedback systems. In those applications, it is assumed that there is no input to the system-that is, only the initial condition is considered. We will use this assumption in the system shown in Figure 1.2; furthermore, we will assume that the element $G(.)$ that follows the nonlinearity is effectively low-pass, which is common to the power-output device of a

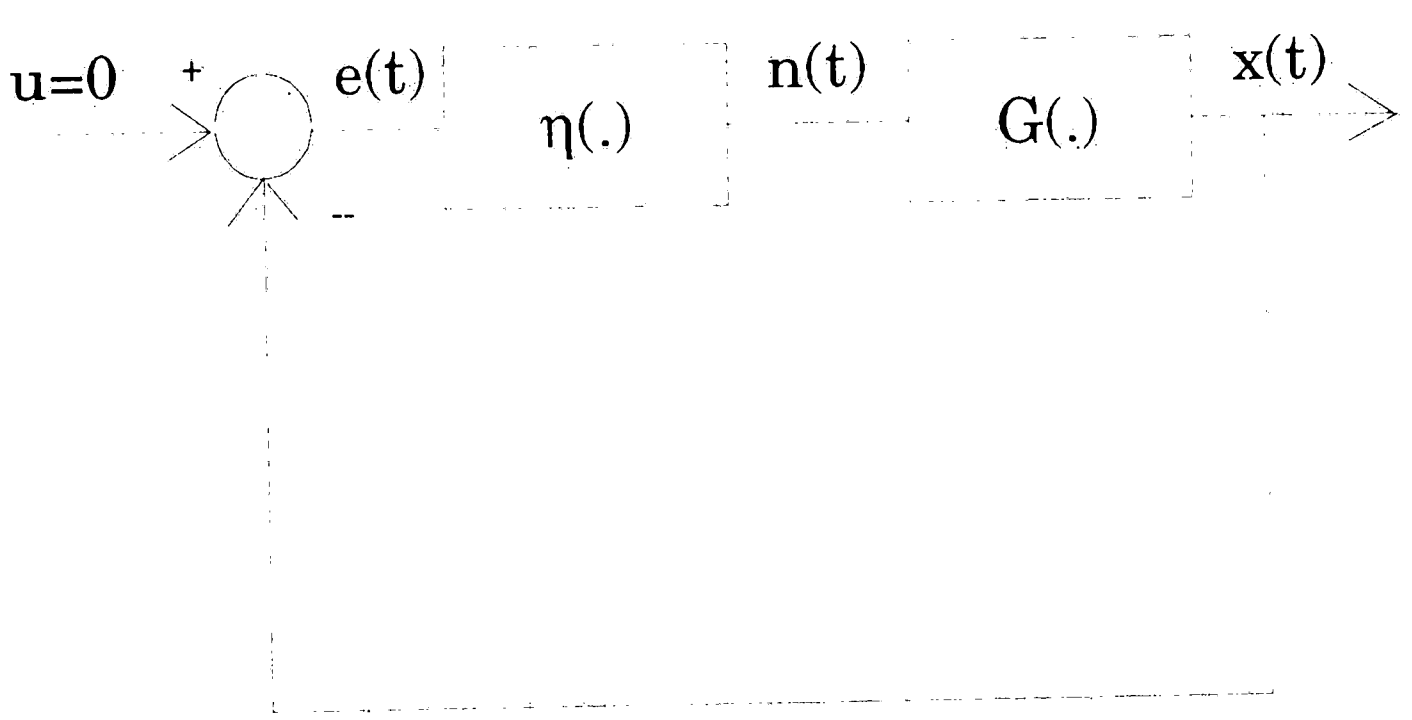

Figure 1-2: An oscillator system.

control system which attenuates the higher harmonics of a periodic waveform much more strongly than the fundamental. Let us consider the error signal $e(t)$ which is the input to the nonlinearity to be sinusoidal, that is,

$$e(t) = V\cos\omega t \tag{1.7}$$

The steady-state output of the nonlinearity is expected to be periodic and nonsinusoidal. Representing the output by it's Fourier series, we have

$$n(t) = \frac{A_0}{2} + \sum_{k=1}^{\infty} (A_k \cos k\omega t + B_k \sin k\omega t) \tag{1.8}$$

Where the Fourier coefficients are given by

$$A_k = \frac{2}{T}\int_{t_0}^{t_0+T} n(t)\cos k\omega t dt \tag{1.9}$$

$$B_k = \frac{2}{T}\int_{t_0}^{t_0+T} n(t)\sin k\omega t dt \tag{1.10}$$

where $T = \frac{2\pi}{\omega}$ is the period of the input sinusoid e(t) and t_0 is an arbitrary value of time. We will consider the case where the nonlinearity is odd, which gives us $A_0 = 0$. Since we have established that $G(.)$ is low-pass and will effectively filter the higher harmonics of $n(t)$, the output can be expressed as follows:

$$x(t) \approx C\cos(\omega t + \theta) \tag{1.11}$$

Since the higher harmonics of $n(t)$ have little effect on the output, they can be ignored with little consequence. Now (1.8) becomes

$$n(t) \approx A_1 \cos\omega t + B_1 \sin\omega t \tag{1.12}$$
$$n(t) = N_1 \cos(\omega t + \phi)$$

Where $N_1 = \sqrt{A_1^2 + B_1^2}$ and $\phi = -\arctan\frac{B_1}{A_1}$. Therefore the gain of the

nonlinearity can be expressed as follows:

$$\eta(V,\omega) = \frac{N_1 e^{j\phi}}{V} \tag{1.13}$$

The gain $\eta(V,\omega)$ is the describing function of the nonlinearity. In this case, the describing function $\eta(V,\omega)$ is the transfer function relating the input sinusoid to the first harmonic of the output. The procedure deriving it is also called the *principle of harmonic balance*. Static systems generally have a describing function which is a function only of the amplitude of the input, but dynamic systems-for example, where the output and input are related through a nonlinear differential equation-will have a describing function which is a function of both the amplitude and the frequency of the input. General formulas for the describing functions of a wide class of nonlinearities has been developed by Sridhar [9]. For the oscillator circuit in Figure 1.2, the error signal can be expressed as follows:

$$e(t) = -x(t) \tag{1.14}$$

Equating the phasors of (1.14) we have

$$\begin{aligned} V &= -G(j\omega)\eta(V,\omega)V \\ 1 &= -G(j\omega)\eta(V,\omega) \end{aligned} \tag{1.15}$$

If a limit cycle exists for a particular frequency, ω, the value of V in (1.15) can be found.

The describing function technique has proven to be an effective analytical tool in the area of nonlinear systems. In this study, the concept of the describing function is used in a numerical algorithm that can analyze a wide range of nonlinear circuits. The next chapter discusses the harmonic balance method, an extension of the

describing function technique in which multiple harmonics are included in the analysis, and the numerical solution that is introduced in this study which is coined as "The Generalized Describing Function Method".

Chapter 2
Numerical Solution in the Frequency Domain

Numerical techniques utilizing the digital computer have been used extensively in the study of nonlinear circuits. Some of the most popular numerical algorithms include the Newton-Raphson, the Runge-Kutta, and the various predictor-corrector methods. These and other algorithms are discussed comprehensively in the book by Chua and Lin [10]. In this chapter, a numerical method called the *Generalized Describing Function Method* will be introduced, and from here on will be referred to as the GDF. The GDF is an iterative numerical scheme based on the basic principle that was introduced in the preceding chapter, that of approximating the transfer characteristics of a nonlinear element with a linear time-invariant operator. The GDF is a frequency domain algorithm, as opposed to the methods mentioned above which are based on the time domain. A good portion of the set of equations that define the GDF algorithm can be implemented using the program SPICE, a reliable and well-documented simulator for linear circuits. Two distinctive advantages are gained from the capability of the GDF to use the program, SPICE, as it's front end tool: from the programmer's point of view, it eliminates programming an algorithm from its roots; and from the user's, it allows one to analyze a wide range of nonlinerities.

We will begin our discussion by introducing the principle of

harmonic balance, where the nonlinearity is approximated by a filter function; hence, harmonics are being carried over in the iterative solution.

2.1 Harmonic Balance

The method of approximation using harmonic balance was developed for nonlinear periodic networks in order to avoid the time domain solution of dynamic equations [4]. The differential equations are converted into nonlinear algebraic equations that can be solved for a periodic steady-state solution, then computation is carried out in the frequency domain [11]. Our purpose here is not to probe deeply into the theory of harmonic balance, but rather to use it to introduce the GDF, which is a close variation of the method. Our approach; therefore, is to develop equations that will build into a numerical algorithm that can be implemented by the computer.

It has been shown by Frey [12] that general nonlinear networks composed of both resistive and reactive nonlinearities can be represented by

$$x = Au + BF(x) \tag{2.1}$$

where x is generally a vector composed of tree branch voltages and link currents, u is a vector of independent sources, A and B are matrices composed of components which are constants or linear operators, and $F(x)$ is a mapping of $R^k \rightarrow R^k$. For the purposes of our discussion; however, we will limit ourselves to only one independent source u, with $F(x)$ representing the nonlinearity, and x will be

considered as the output.

The concept of linear approximation can be illustrated in the simplified geometric representation shown in Figure 2-1a. The nonlinearity $F(x)$ is approximated by a line that intersects it at one point, and the x coordinate of this point is the response. In the formulation of our equations, we will explicitly include the *y–intercept* of the line as shown in Figure 2-1b, represented as F_y, the implication of which will be given later. The principle is represented as follows:

$$F(x) \approx F_y + \lambda \bar{x} \tag{2.2}$$

where λ is the slope.

For a sinusoidal input, $F(x)$ will generate a nonsinusoidal output and at steady-state can be represented by its Fourier series. Since $F(x)$ has the effect of producing harmonics in its output, proper modeling can be done by making the linear operator λ a filter function, producing sinusoids that effectively balance the harmonics of the actual nonlinear output. λ can now be broken down, as follows:

$$\lambda = \sum_{i=1}^{N} \lambda_i L_i(\omega) \tag{2.3}$$

where λ_i are weights operating on the filter function $L_i(\omega)$. Substituting (2.2) into (2.1) yields

$$\bar{x} = Au + BF_y + B\lambda\bar{x} \tag{2.4}$$

and the error of the approximation is seen to be

$$e = x - \bar{x} \tag{2.5}$$

The error can be minimized by optimizing λ. This involves using a

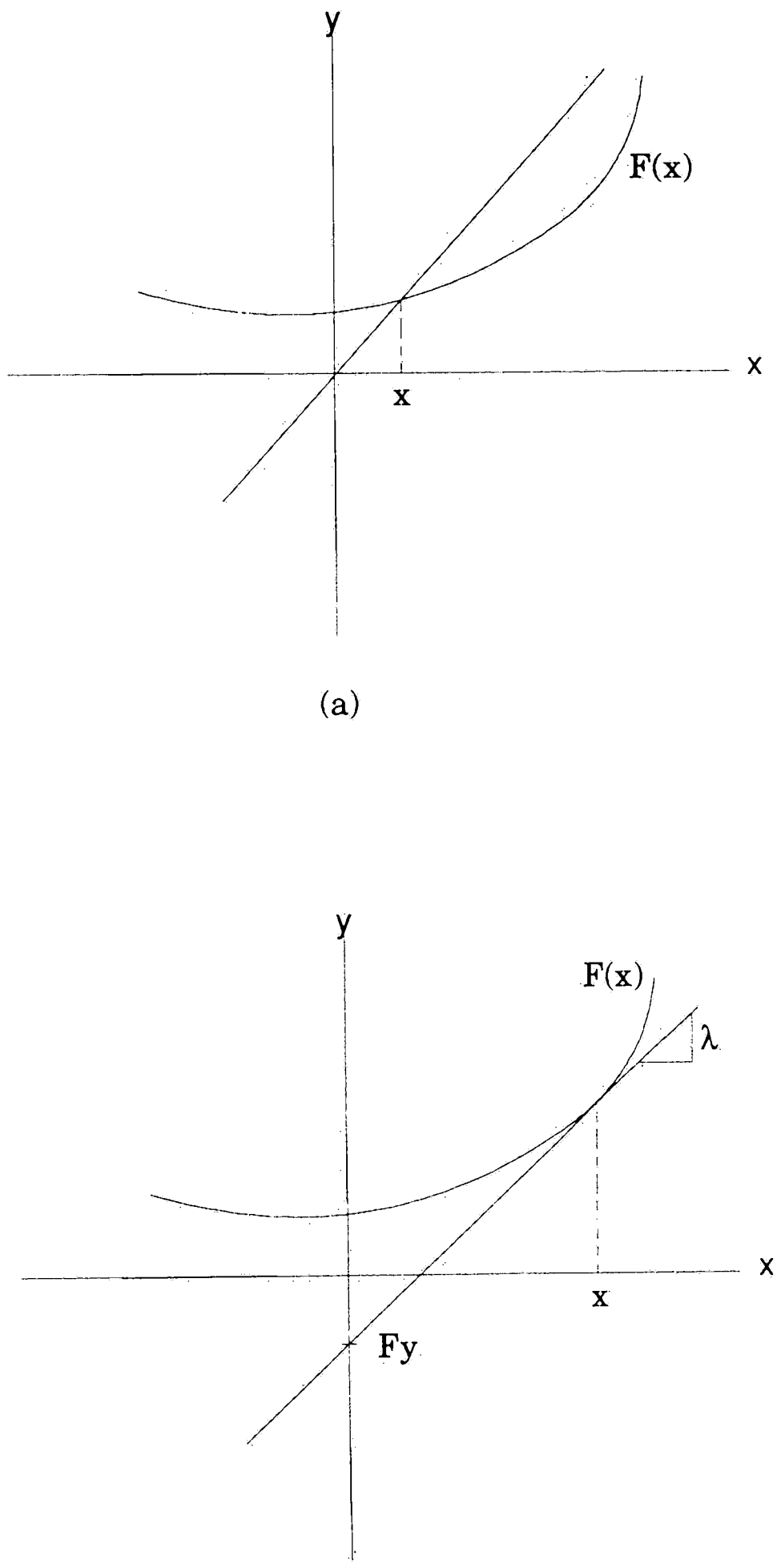

(a)

(b)

Figure 2-1: Approximating F(x) with a line.

reasonable initial value for λ and updating the value by successive approximation. Optimization of λ is then realized by making the ratio of the change in the mean squared error to the change in λ to approach to zero. This concept is put into equation form as follows:

$$\frac{d\|e\|^2}{d\lambda_i} = 2<e, \frac{de}{d\lambda_i}> = 0 \tag{2.6}$$

where the operator <., .> represents the inner product.

For the purpose of our next discussion, let us denote:

$$d\|e\|^2 = f(\lambda_1, \lambda_2, .., \lambda_N)$$

and

$$\frac{\partial f}{\partial \lambda_i} = f_i'$$

Suppose

$$f_i'(\lambda_1 + \Delta\lambda_1, \lambda_2 + \Delta\lambda_2, .., \lambda_N + \Delta\lambda_N) = 0 \tag{2.7}$$

Expanding (2.7) by taking the first two terms of it's Taylor series, we have as follows:

$$f'(\lambda_1, \lambda_2, .., \lambda_N) + J(\Delta\lambda_1, \Delta\lambda_2, .., \Delta\lambda_N)^T = 0 \tag{2.8}$$

where J is the Jacobian matrix in the form:

$$J = \begin{vmatrix} g_{11} & g_{12} & . \\ g_{21} & . & \\ . & & \end{vmatrix}$$

where

$$g_{11} = \frac{\partial^2 f}{\lambda_1 \lambda_1}, \quad g_{12} = \frac{\partial^2 f}{\lambda_1 \lambda_2}, \quad g_{21} = \frac{\partial^2 f}{\lambda_2 \lambda_1}, \; etc.$$

Suppose J is a diagonal matrix, we have

$$\Delta\lambda = -J^{-1} f' \tag{2.9}$$

and

$$\Delta\lambda_i = -\frac{\partial f}{\partial \lambda_i}\left(\frac{\partial^2 f}{\partial \lambda_i^2}\right)^{-1}$$

The evaluation of (2.9) will give us the change in λ_i for each iteration. Here $\frac{\partial f}{\partial \lambda_i}$ has the value given in (2.6). We then get the derivative of (2.6) with respect to λ_i resulting in

$$\frac{\partial^2 f}{\partial \lambda_i^2} = \frac{d^2 \| e \|^2}{d\lambda_i^2} \tag{2.10}$$

$$\frac{\partial^2 f}{\partial \lambda_i^2} = 2\left(<\frac{de}{d\lambda_i}, \frac{de}{d\lambda_i}> + <e, \frac{d^2 e}{d\lambda_i^2}>\right)$$

Evaluating the variables in (2.10), starting with e where we substitute the values of x and $\bar{x}$ from (2.1) and (2.4)into (2.5), yields

$$e = B(F(x) - F_y - \lambda\bar{x}) \tag{2.11}$$

or

$$e = B(F(x) - F_y - \lambda x) + B\lambda e$$

Taking the derivative of (2.5) with respect to λ_i will result in the following sequence of equations:

$$\frac{de}{d\lambda_i} = \frac{dx}{d\lambda_i} - \frac{d\bar{x}}{d\lambda_i}$$

Since x is not a function of λ, we eliminate the first term. Substituting (2.4) into the second term we get

$$\frac{de}{d\lambda_i} = -\frac{d(Au+F_y)}{d\lambda_i} + \frac{d}{d\lambda_i}(B\sum_{i=1}^{N}\lambda_i L_i)$$

The numerator of the first term does not change with respect to λ, which makes it equal to zero, leaving the second term to evaluate into

$$\frac{de}{d\lambda_i} = -B[L_i x + \sum_{i=1}^{N}\lambda_i L_i \frac{d\bar{x}}{d\lambda_i}]$$

Inserting λ into the equation from its expression from (2.3), we have as follows:

$$\frac{de}{d\lambda_i} = -BL_i\bar{x} - B\lambda\frac{d\bar{x}}{d\lambda_i} \tag{2.12}$$

or

$$\frac{de}{d\lambda_i} = -BL_i\bar{x} + B\lambda\frac{de}{d\lambda_i}$$

Consequently getting the derivative of (2.12) with respect to λ_i will result in

$$\frac{d^2e}{d\lambda_i^2} = -BL_i\frac{d\bar{x}}{d\lambda_i} + BL_i\frac{de}{d\lambda_i} + B\lambda\frac{d^2e}{d\lambda_i^2} \tag{2.13}$$

or

$$\frac{d^2e}{d\lambda_i^2} = -2BL_i\frac{de}{d\lambda_i} + B\lambda\frac{d^2e}{d\lambda_i^2}$$

Note that (2.4), (2.11), (2.12), and (2.13) can be expressed in closed form, but we will leave it in it's present form for the purpose of computer implementation, which will be discussed in the next chapter. The equations that have been derived above will be arranged to form a numerical algorithm and will be presented in the

next section.

2.2 The Generalized Describing Function(GDF) Method

The GDF is a variation of the harmonic balance and is based on the simplifying assumption that

$$L_i = 1 \tag{2.14}$$

and

$$\lambda_i = \lambda_1$$

for all i

What makes the GDF an extension of the classical describing function method is that we can generate higher harmonics with the use of F_y; thereby, significantly increasing the accuracy of the approximation for circuits with large harmonic distortion while keeping the level of complexity at a manageable level. This scheme of generating harmonics will become evident when we cover circuit modeling in the next chapter. For the purpose of our discussion of the GDF algorithm, and based on our assumption in (2.14) we can drop L_i from the equations and make $\lambda_i = \lambda$. The superscripts in our variables indicate the iteration number. The GDF algorithm is described in the following steps:

1. Make the initial guess x and call it $\bar{x}^0$. The initial value of λ will then be solved by getting the instantaneous slope of $F(x)$ at point $\bar{x}^0$ (see Figure 2-1), that is

$$\lambda^0 = F'(\bar{x}^0)$$

2. Solve for F_y by using (2.2), that is

$$F_y^0 = F(\bar{x}^0) - \lambda^0 \bar{x}^0$$

3. Our next step would be to solve $\bar{x}^1$ by using (2.4), that is

$$\bar{x}^1 = Au + BF_y^0 + B\lambda^0 \bar{x}^1$$

4. Having determined the value for $\bar{x}^1$, we can solve for $\Delta\lambda$ which is then used for determining the next value for λ by: $\lambda^1 = \lambda^0 + \Delta\lambda$, that is, by using (2.9), (2.6), (2.10), (2.11), (2.12), and (2.13) as follows:

$$\Delta\lambda = -\frac{\partial f}{\partial \lambda^0}\left(\frac{\partial f}{\partial \lambda^2}\right)^{-1}$$

from (2.9) and

$$\frac{\partial^2 f}{\partial \lambda} = 2\langle e, \frac{de}{d\lambda}\rangle$$

from (2.6), also

$$\frac{\partial^2 f}{\partial \lambda^2} = 2\left(\langle \frac{de}{d\lambda}, \frac{de}{d\lambda}\rangle + \langle e, \frac{d^2 e}{d\lambda^2}\rangle\right)$$

from (2.10), where the variables from above can be evaluated by

$$e = B(F(\bar{x}^1) - F_y - \lambda^0 \bar{x}^0) + B\lambda^0 e$$

$$\frac{de}{d\lambda} = -B\bar{x}^1 + B\lambda^0 \frac{de}{d\lambda}$$

$$\frac{d^2 e}{d\lambda^2} = -2B\left(\frac{de}{d\lambda} + B\lambda^0 \frac{d^2 e}{d\lambda^2}\right)$$

from (2.11), (2.12), and (2.13) respectively.

5. Go back to step 2, to solve for F_y^1.

The computer implementation of this algorithm will be discussed in the next chapter, where we incorporate the circuit simulator SPICE into the computation. Other computational issues

like sampling, Fourier transform evaluation and inner product will also be discussed.

Chapter 3
Computational Issues

One of the most important criteria in judging the effectiveness of a numerical algorithm is it's suitability for computer implementation. As previously discussed, time domain based algorithms are computationally expensive for long transient conditions. The advantage of the GDF over other frequency domain algorithms on the other hand are: it's simplicity for computer implementation; and it's flexibility afforded by the capability to use SPICE. If the reader is not familiar with SPICE, refer to [13] and [14]. There is a version of SPICE that runs on a microcomputer called PSPICE and is documented in [15]. The choice of which version to use will depend on the working environment where the study is being made. The data used in this paper has been gathered using PSPICE. The feature of SPICE that is used is the AC analysis, which gives the steady-state frequency response as it's output. Any other circuit simulator having the same feature can also be used. The first section of this chapter decribes the role of SPICE in one form of implementation of the GDF algorithm-which is the one used in this study, while the second section discusses the software issues.

3.1 Role of SPICE AC analysis

The AC analysis (also called frequency response analysis) procedure is used to calculate node voltages and branch currents over a swept range of frequencies. It is a small-signal analysis, where the circuit has already achieved steady state; therefore, the circuit is assumed to be free from transient and large-signal nonlinearities. The AC analysis outputs the amplitude and phase angles of the node and branch currents and it is also possible for the output to be expressed in complex form, giving the results in terms of real and imaginary components. Our first objective would be to arrange the circuit so that it can be expressed in the form of (2.1). Then we will model the nonlinear component $F(x)$ with a linear equivalent as in (2.2), and since the circuit will now contain all linear elements, we can set them up in the SPICE input card.

We will use the circuit shown in Figure 3-1a to introduce the role of SPICE in our GDF implementation. From the constitutive equation of the nonlinerity as shown in Figure 3-1a, we can split it into a linear and nonlinear part as shown in Figure 3-1b, Where the nonlinearity $F(x)$ is represented by a voltage-controlled current source. We then write the circuit equation and express it in the form of (2.1), that is

$$x = Au + BF(x)$$

where

$$A = \frac{sCR_0}{1+sCR_0}$$

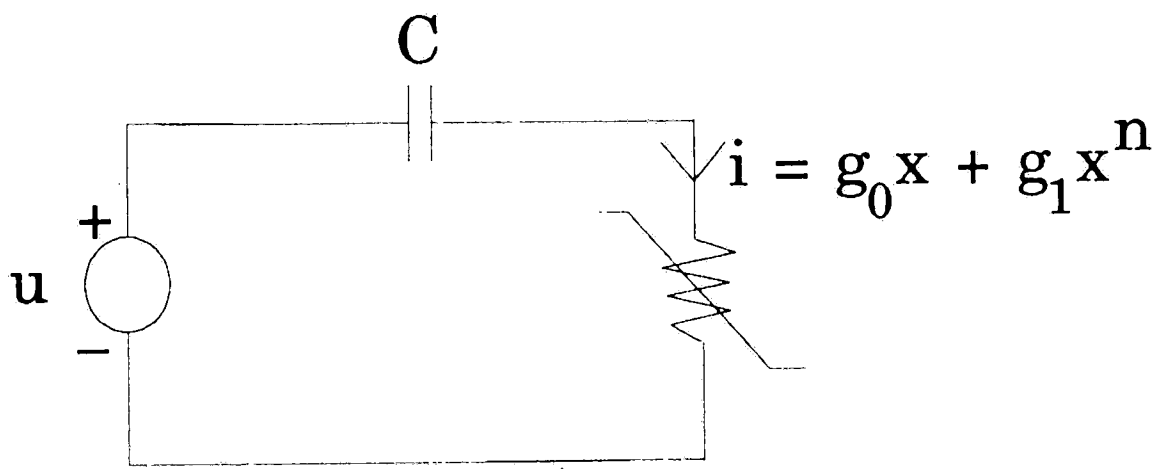

(a)

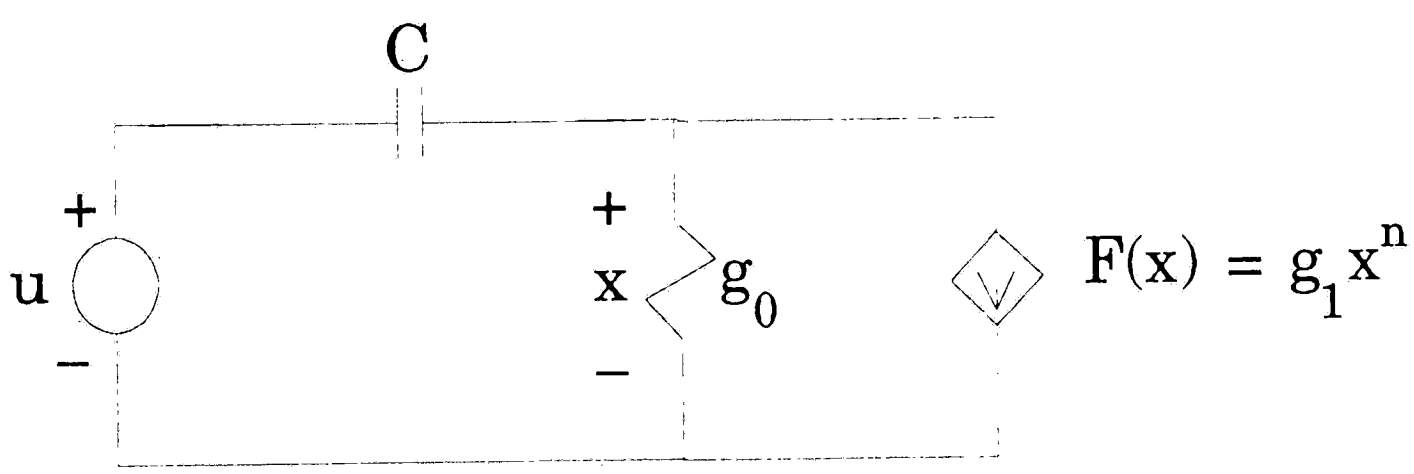

(b)

Figure 3-1: Modeling the nonlinear component.

and

$$B = \frac{-R_0}{1+sCR_0}$$

where we have used $R_0 = 1/g_0$. The linearized equivalent of the circuit is shown in Figure 3-2a, and in Figure 3-2b, where the nonlinear element is split into an independent source F_y and a voltage-controlled current source $\lambda\bar{x}$ so that the circuit equation can be written in the form of (2.4), that is

$$\bar{x} = Au + BF_y + B\lambda\bar{x}$$

where the values for A and B are the ones given above. Note that λ can be complex; therefore, proper modeling is necessary. An example of how $\lambda\bar{x}$ is modeled is outlined in the software documentation. The availability of this documentation is given in the next section. After proper modeling has been done on $\lambda\bar{x}$, and after having computed the values for λ and F_y using steps 1 and 2 of the GDF algorithm, the circuit would now be ready to be set up into the SPICE input card.

3.1.1 Solution Using the Fundamental Harmonic

If we assume that we carry only the fundamental harmonic of the output of the nonlinearity-*i.e.*, as in the describing function method-we can get the value of the voltage (or current) $\bar{x}$ from the output of the AC analysis, and this value would be at the same frequency as the input source u.

The discussion above has covered the first three steps of the GDF algorithm; however, the role of the SPICE AC analysis still extends to step 4-that is, in solving for $\Delta\lambda$ in (2.9). Recalling the

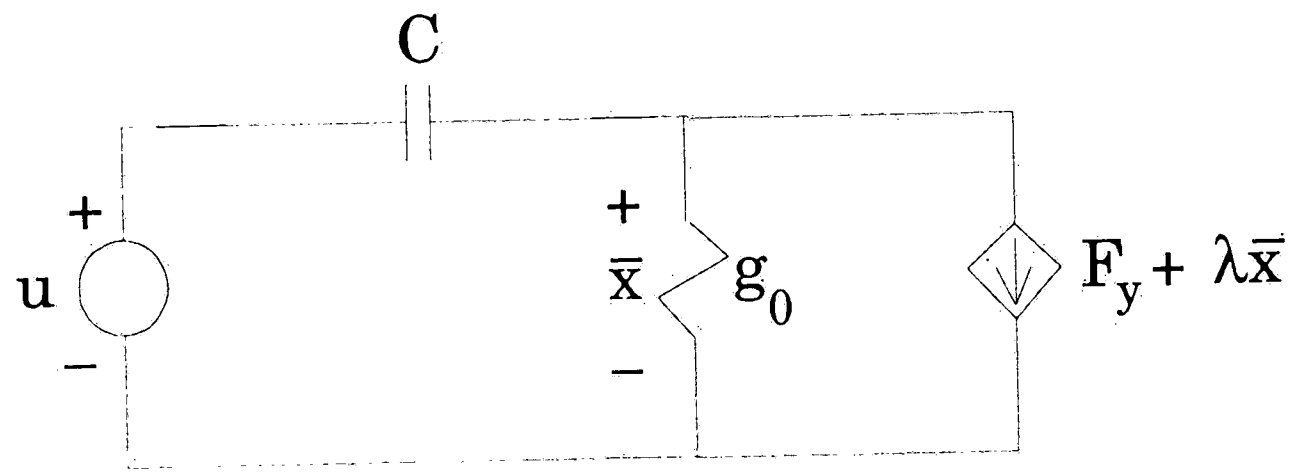

(a)

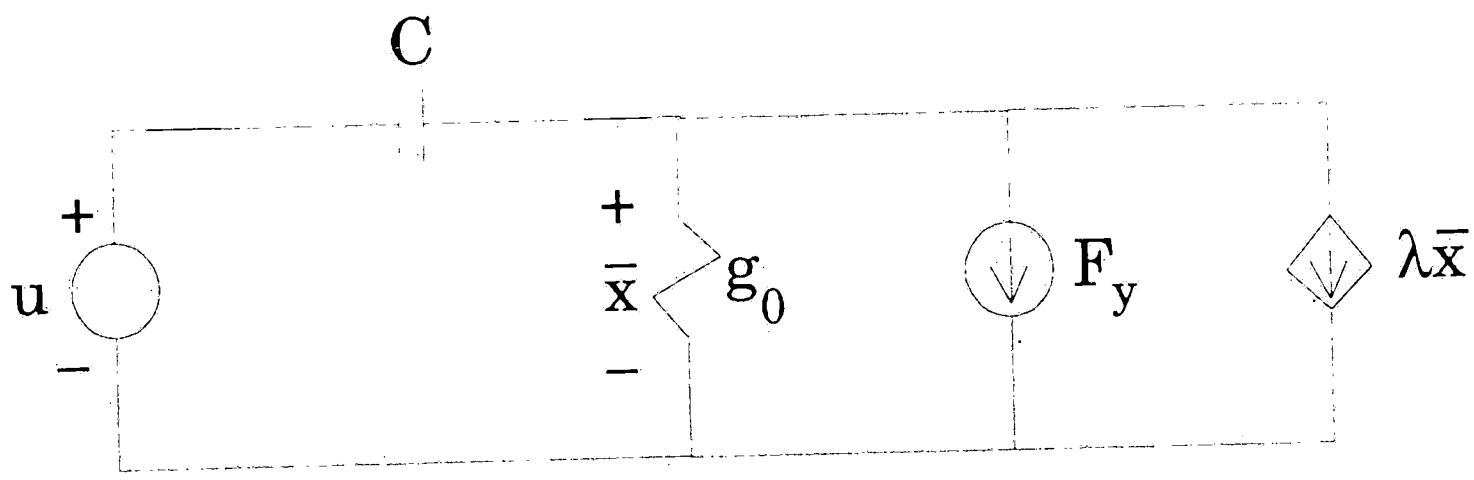

(b)

Figure 3-2: Splitting the controlled source.

equations from step 4 which are (2.11), (2.12) and (2.13), they are respectively:

$$e = B[F(\bar{x}) - F_y - \lambda\bar{x}] + B\lambda e$$

$$\frac{de}{d\lambda} = -B\bar{x} + B\lambda\frac{de}{d\lambda}$$

$$\frac{d^2e}{d\lambda^2} = 2B\frac{de}{d\lambda} + B\lambda\frac{d^2e}{d\lambda^2}$$

If we examine the structure of these three equations, and compare it with (2.4), we immediately notice their parallelism. Comparing (2.4) and (2.11) for example; if we replace $\bar{x}$ and F_y in (2.4) with e and $F(\bar{x}) - F_y - \lambda\bar{x}$, while letting $Au = 0$, we get (2.11). That means we can use the same circuit shown in Figure 3-2b, replacing the independent source F_y with $F(\bar{x}) - F_y - \lambda\bar{x}$ and letting $u = 0$, run SPICE again, and the output will give the value for e. Replacing F_y with $-\bar{x}$ and $2B\frac{de}{d\lambda}$ and running SPICE each time, would give $\frac{de}{d\lambda}$ and $\frac{d^2e}{d\lambda^2}$ respectively.

3.1.2 Extension to Higher Harmonics

We have assumed so far that only the fundamental is at the output of the nonlinearity and neglected the higher harmonics; however, using SPICE, the GDF can also carry over the higher harmonics, which is necessary in the case when the circuit has a large harmonic distortion. It is possible in the SPICE AC analysis to set the values of the independent sources for a sweep of frequencies. Since the nonlinearity $F(x)$ has been split into an independent source F_y and a controlled source $\lambda\bar{x}$, if we want to include the harmonics at the output of the nonlinearity, we have to set the values of F_y for a

sweep of frequencies, *e.g* ω_1, $2\omega_1$, $3\omega_1$, etc. In this event, SPICE will now model F_y as a superposition of several independent sinusoidal sources in parallel (or in series), as shown in Figure 3-3, in which the frequencies of these sources are harmonically related. The fundamental of F_y has the same frequency as the input u. However, since the input does not contain harmonics, we have to run SPICE twice: first with $F_y = 0$, with the result containing only the fundamental; then run it again with $u = 0$, where in this case the result contains both fudamental and harmonics. We use superposition on these results to get the value of $\bar{x}$, which will now be for a sweep of frequencies. Since we have four equations, (2.4), (2.11), (2.12), and (2.13) to compute, we will have to run SPICE eight times for each iteration of $\Delta\lambda$. There is a way out of this dilemma; however, referring to Figure 3-4. We can obtain the transfer function $H(\omega_1)$ with respect to u by making the input $u_T = 1$, the output of SPICE will then be equal to $H(\omega_1)$. Using the same procedure, we are able to get the transfer function $G(\omega)$ with respect to F_y by making the input $(F_y)_T = 0$. An example of how this is set up it the input card is shown in the software documentation. Also shown is the PSPICE output file, where the real and imaginary components are shown with the corresponding frequencies. A different command in the input card can also show the output in terms of the magnitude and the phase, also formatted with it's frequency. Consequently, we compute for $\bar{x}$, e, $\frac{de}{d\lambda}$ and $\frac{d^2e}{d\lambda^2}$ by

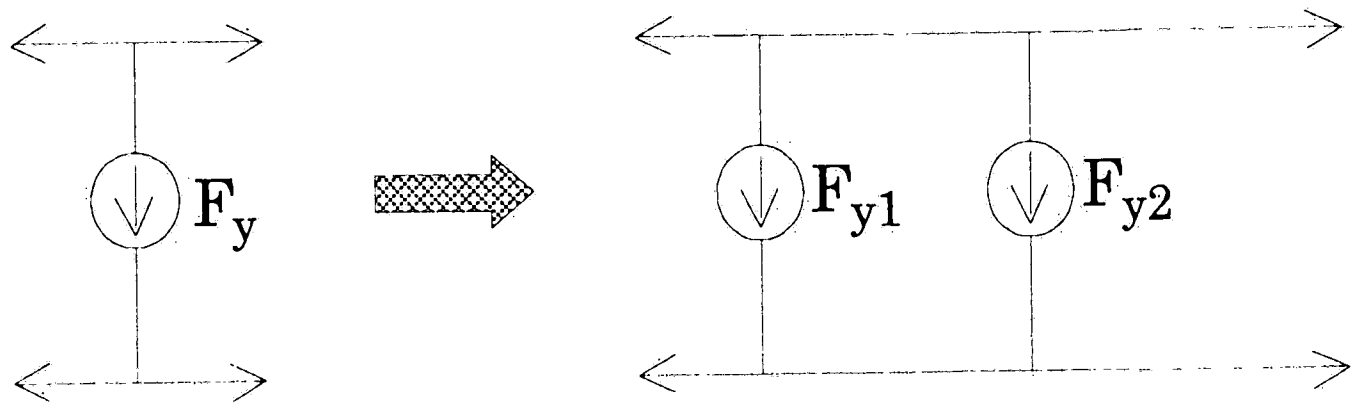

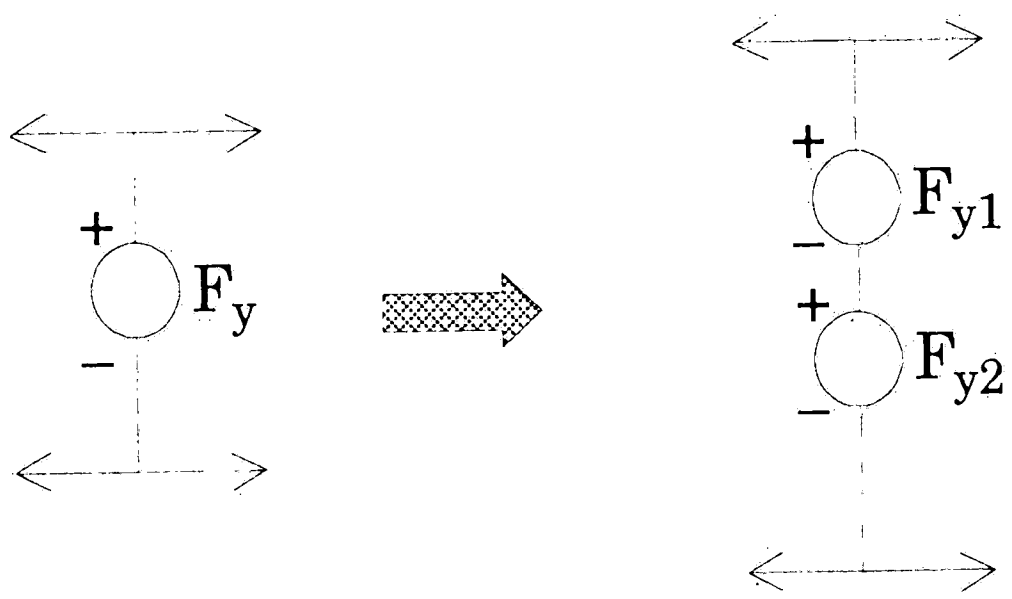

Figure 3-3: Generating harmonics using F_y.

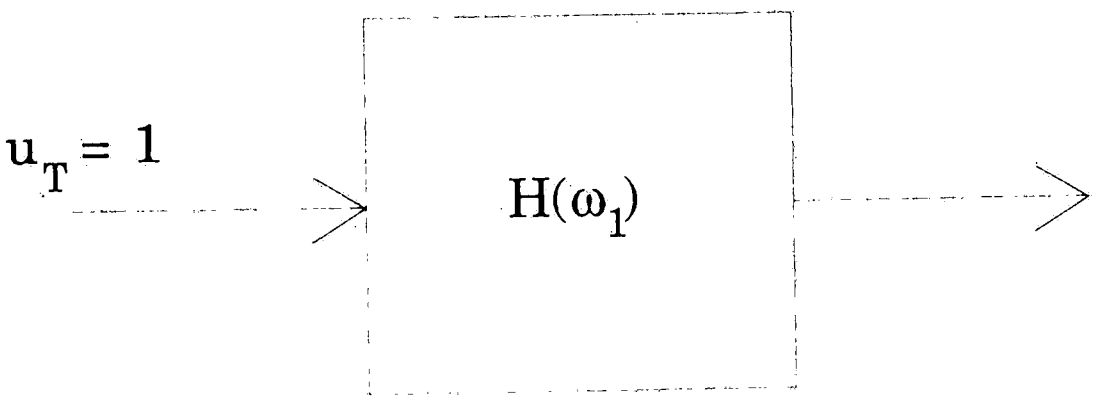

Figure 3-4: Solving for the transfer function using a unity input.

$$\bar{x}(\omega) = uH(\omega_1) + F_y(\omega)G(\omega) \tag{3.1}$$

$$e(\omega) = [F(\bar{x}(\omega)) - \lambda\bar{x} - F_y(\omega)]G(\omega) \tag{3.2}$$

$$\frac{de}{d\lambda}(\omega) = -\bar{x}(\omega)G(\omega) \tag{3.3}$$

$$\frac{d^2e}{d\lambda^2}(\omega) = 2\frac{de}{d\lambda}(\omega)G(\omega) \tag{3.4}$$

Using this procedure, we can observe that instead of running SPICE eight times for each computation of $\Delta\lambda$, we only run it twice!

3.2 Software Implementation

The computer implementation that was used to gather data for this paper is discussed in this section. Although, the use of software engineering terminology is inevitable when we touch programming concepts, we will proceed with the discussion without any reference to a specific computer language, keeping the focus on the issues that will affect the accuracy of the data being generated. The computation of Fourier transforms and inner products are discussed in detail, and possible sources of errors are acknowledged. The philosophy that was used in the design of the programs is to make them reusable for future extensions, a notable possibility is the harmonic balance method. Object-oriented concepts, like modularity, and information hiding have been applied so that portions of the programs can be extracted for research in closely related fields later on. The software containing source codes and executables used in this study filed on

disks with a short documentation included, are available from Professor Douglas R. Frey of the Computer Science and Electrical Engineering Department, Lehigh University.

3.2.1 Program Flow

The control flow of the implemented GDF algorithm, which we will refer to as "program GDF" is summarized on the flowchart in Figure 3-5. Program GDF is made into a parent process, with three programs which are automatically called as child processes, and they are: the PSPICE; program Read Spice; and program Delta Lambda. The editor, which is used to edit the PSPICE input card can also be made into a child process, or can be done interactively in case the user wants to study the output files at the end of each iteration. Another observation that can made is that the routines of program Read Spice can be absorbed into program Delta Lambda; however, it is kept separate because it is a general program which can be used by any other program that needs to read the output of PSPICE. We will go through the blocks of the flowchart sequentially. The preprocessing portion involves entering the initial values of λ and F_y into a data file which will be read by program Delta Lambda during its execution. Also entered in the data file is the value of the input signal. The next step involves the preparation of the PSPSICE input card, in which, after the first iteration, only the value of λ will be edited. PSPICE will now be run automatically twice by the program GDF, and outputs $H(\omega_1)$ and $G(\omega)$. program Read Spice will be executed next, which will just screen the output file of PSPICE and

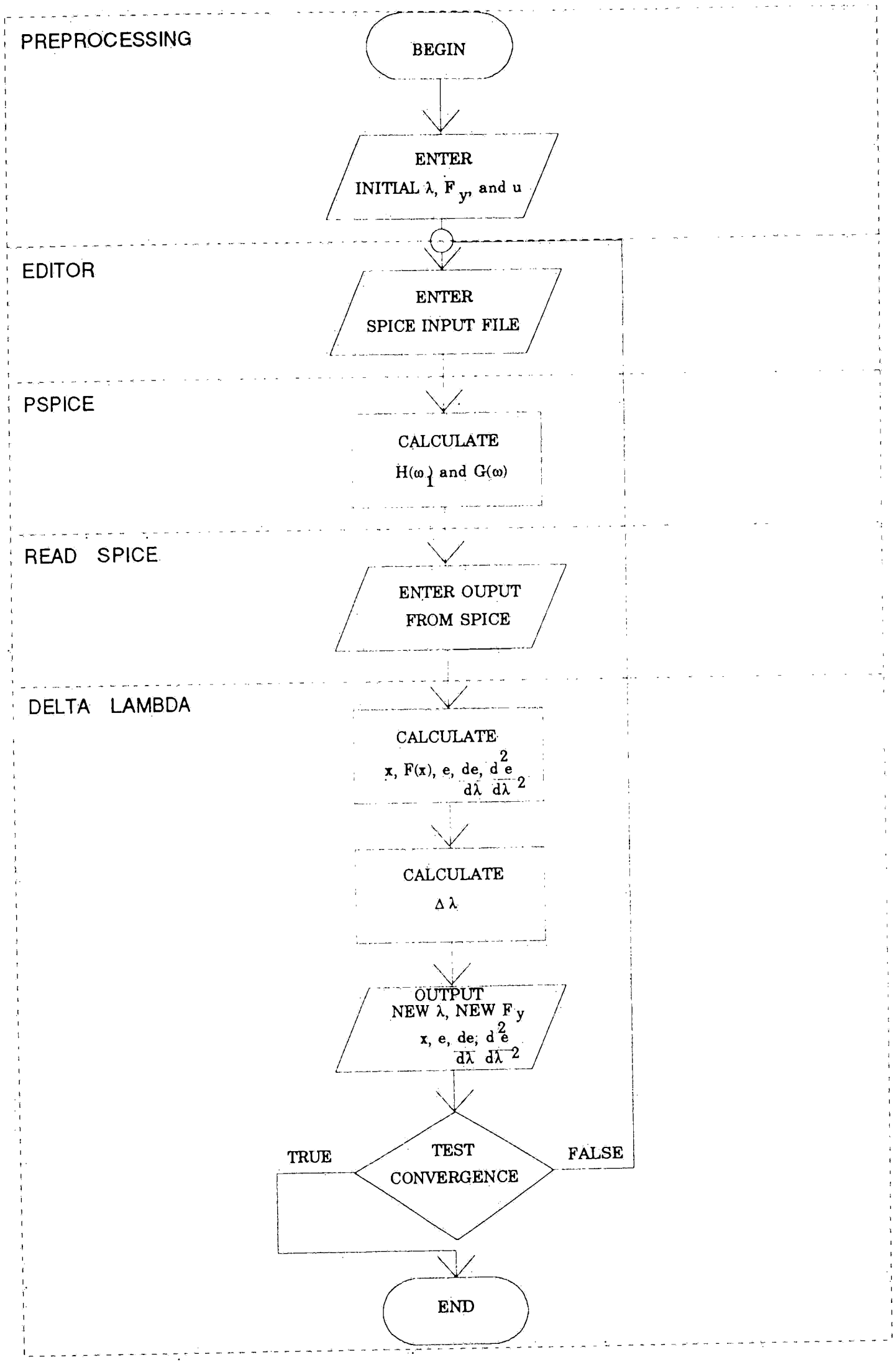

Figure 3-5: Flowchart of the GDF algorithm as implemented.

extracting only the necessary data, put it into files that will be read by program Delta Lambda, which will then do all the calculations in order to arrive at the value for $\Delta\lambda$. The computation of $F(\bar{x})$ requires special attention because it the involves the Fourier transformation from the time domain representation to frequency domain, which is the necessary form of the data. This will be discussed in detail in a subsection below. The program Delta Lambda will output the new values of λ and F_y to the data file. The values of the error, the derivative of the error and the second derivative of the error is outputed to an error file. The data file and the error file are therefore updated after each iteration. The determination of convergence, which is the last step, is discussed below. A tree diagram of the data structure, and a summary of all the data and file structures and routines used in program Delta Lambda are given in the software documentation.

3.2.2 Truncated Fourier Series

Since we have established the assumption that the input must be sinusoidal, the output signal represented as $\bar{x}(\omega)$ is periodic and generally nonsinusoidal, composed of sinusoidal components in the form of it's fundamental and harmonics. It is always assumed that the values are complex, that is

$$Re[\bar{x}_1]+Im[\bar{x}_1], Re[\bar{x}_2]+Im[\bar{x}_2], \ldots, Re[\bar{x}_k]+Im[\bar{x}_k]$$

for the respective frequencies: ω_1, ω_2, ..., ω_k, where k is the number of harmonics being carried in the computation. Or expressing it in phasor form

$$\bar{x}_1 e^{j\phi_1}, \bar{x}_2 e^{j\phi_2}, \ldots, \bar{x}_k e^{j\phi_k}$$

As mentioned above, in order to compute for $F(\bar{x})$, we must express this signal in the time domain, that is

$$\bar{x}(t) = \bar{x}_1 cos(\omega_1 + \phi_1) + \bar{x}_2 cos(\omega_2 + \phi_2) + , \ldots, + \bar{x}_k cos(\omega_k + \phi_k) \tag{3.5}$$

This expression is equivalent to a truncated Fourier series. From the mathematical point of view, this is not a complete set of orthogonal basis signals; however, this is a reasonable approximation for a good number of practical circuits where most of the higher harmonics are at the noise level, and therefore, are not a factor in the computation. A graphical example of this approximation is shown in Figure 3-6 for $k = 3$, where the periodic nonsinusoidal signal (shown here for two periods) in Figure 3-6b results after summing three harmonically related sinusoidal signals shown in Fig 3-6a. The computation for the nonlinearity will generate more harmonics for $F(\bar{x})$-for example if the nonlinearity is related to $\bar{x}$through a power of n, that is

$$F[x(t)] = [x(t)]^n$$

The resulting signal will generate a strong nth harmonic, and it's multiples could also be significant. The signal shown in Figure 3-7a is the result of cubing the signal from Figure 3-6b. Signals like this, which result from a nonlinear equation, are almost impossible to express mathematically; hence, in order to compute for the frequency domain representation of such signals (which is what we need), we must resort to a numerical computation, specifically sampling at discrete time points and evaluating the Fourier coefficients. Shown

in Figure 3-7b is the signal from Figure 3-7a being sampled at a window of exactly one period. The window will now be composed of N real sequences $x(mT)$, where T will be dropped from the notation for convenience.

A special mention here with regards to avoiding aliasing is necessary. The highest frequency component that can be represented by sampling will be $\frac{N}{2}$, and since we do not exactly have an idea of the frequency content of $F(\bar{x})$, we must generate the maximum number of samples, without sacrificing computing speed. For the computations that were done for this paper, this was not an issue however, because most of the high frequencies were negligible. Aliasing due to "leakage" is also possible if the sampling window is not exactly one period or a multiple thereof. But again, this has also been carefully avoided.

One way of expressing the sampled nonlinearity $F[x(m)]$ is by a discrete trigonometric Fourier series, which is

$$F[x(m)] = A(0) + \sum_{q=1}^{N/2-1} |A(q)| cos\{\frac{2\pi qm}{N} + tan^{-1}(\frac{Re[A(q)]}{Im[A(q)]})\} + A(\frac{N}{2})cos\pi n$$

where the Fourier coefficients are

$$A(0) = \frac{1}{N}\sum_{m=0}^{N-1} x(m)$$

$$Re[A(q)] = \frac{2}{N}\sum_{m=0}^{N-1} x(m)cos(\frac{2\pi qn}{N})$$

$$Im[A(q)] = -\frac{2}{N}\sum_{m=0}^{N-1} x(m)sin(\frac{2\pi qn}{N})$$

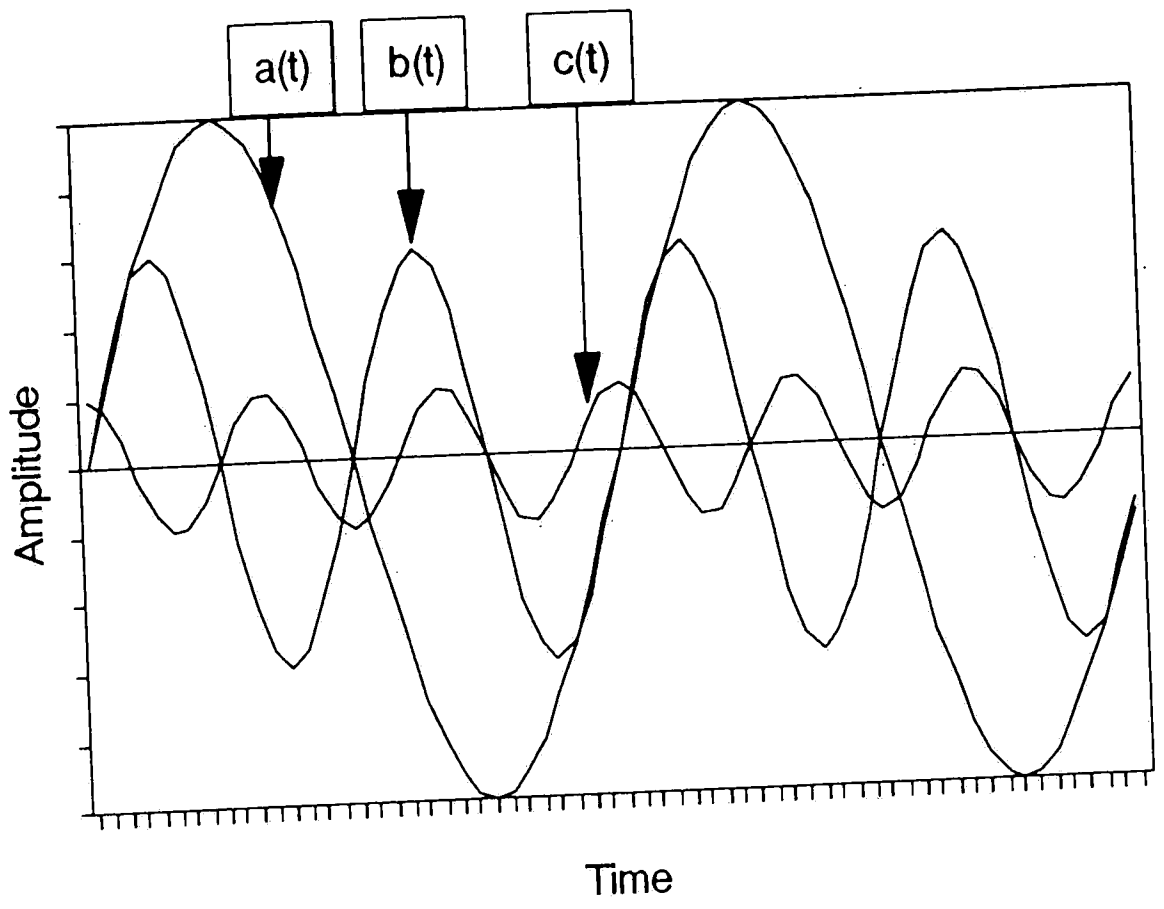

(a)

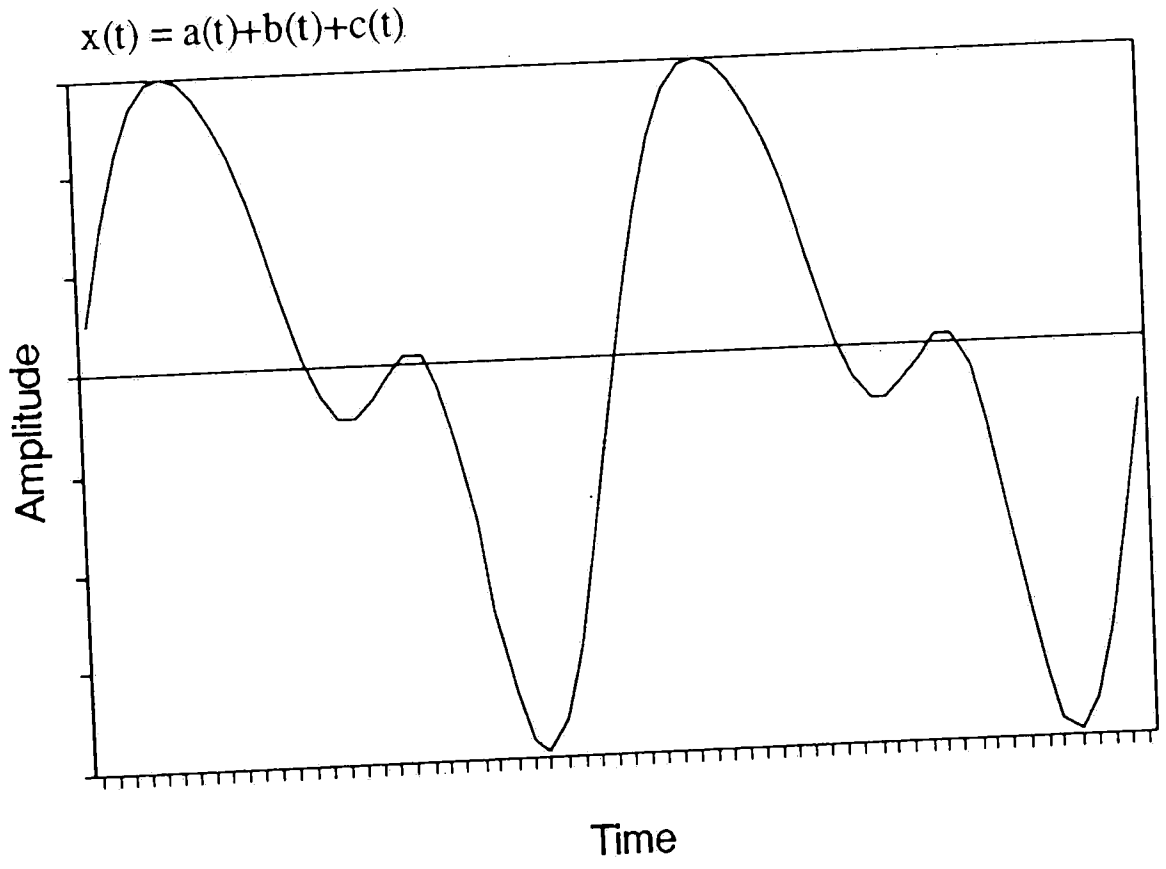

(b)

Figure 3-6: Addition of three sinusoidal signals.

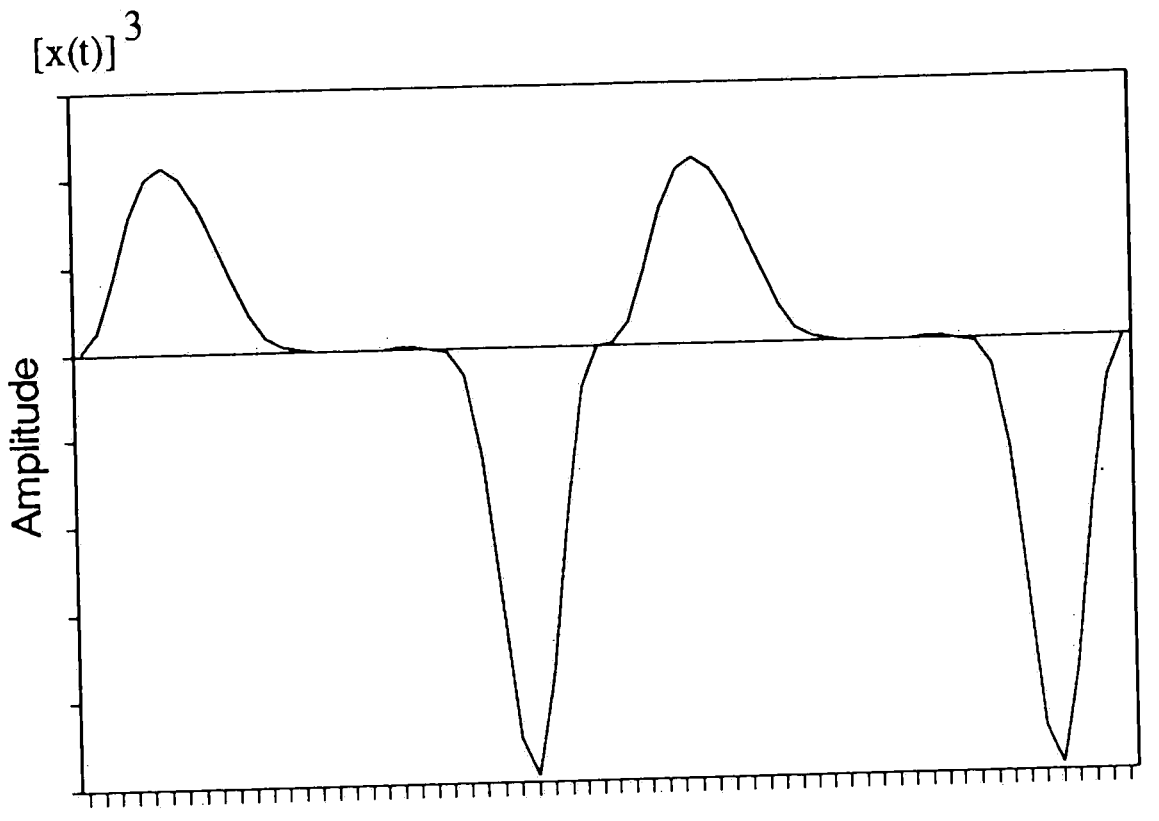

(a)

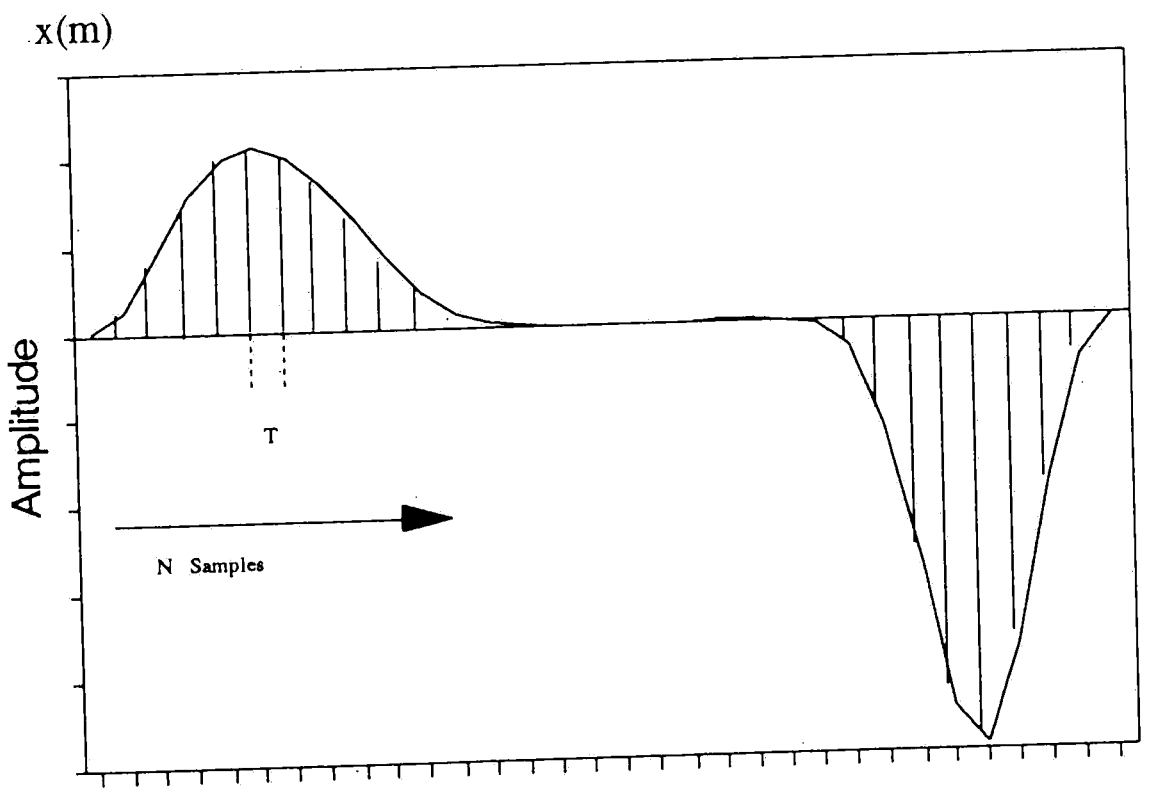

(b)

Figure 3-7: Sampling the signal that resulted from cubing.

$$A(\frac{N}{2}) = \frac{2}{N}\sum_{m=0}^{N-1} x(m)cos\pi n$$

The computation for the Fourier coefficients can be done either by Discrete Fourier Transform (DFT) or by Fast Fourier Transform (FFT), depending on the applicability of either one. The method that is applied in the program Delta Lambda is a DFT. The routine has been written specifically to be a useful part of the program applicable in gathering data for this paper and is not ruesable by itself, and the where the maximum number of samples in relation to speed has been optimized based on experience with the machine used. If the reader is interested, there is a general reusable Fourier transform source code that comes with the disk, and is written using the FFT.

3.2.3 Inner Product

Having covered the method of obtaining the Fourier transform, the next issue to be discussed is the inner product of two signals which is necessary for the computation of $\Delta\lambda$. The inner product of two complex valued signals $y(t)$ and $z(t)$ over the interval (t_1, t_2) is given by

$$<y, z> = \int_{t_1}^{t_2} y(t)z(t)^* dt$$

If the bases that define $y(t)$ and $z(t)$ are finite, they can be represented by their respective Fourier coefficients written as

$$Y_1, Y_2, \ldots, Y_k$$

and

$$Z_1, Z_2, \ldots, Z_k$$

Furthermore, if these two sets of signals are vectors in R^k, then the inner product is computed as follows:

$$<y, z> = Y_1 Z_1^* + Y_2 Z_2^* + , \ldots , + Y_k Z_k^*$$

The variables e, $\frac{de}{d\lambda}$ and $\frac{d^2e}{d\lambda^2}$ can be represented in the same way as $\overline{x}$ in (3.5). Since the fundamental and harmonics of these signals are on the same R^k, the inner product between two of them can be computed as shown above.

3.2.4 Convergence and Sources of Computing Errors

The convergence of the GDF algorithm can be measured using (2.5), that is

$$e = x - \overline{x}$$

when $\frac{de}{d\lambda} \to 0$ we can conclude that we have obtained the best value for x. However, the accuracy of x does not only depend on having $e = 0$, but also on other factors affecting the precision of the computation being carried out. These factors are referred to as truncation errors and rounding errors. Truncation errors happen when digits are dropped from decimal numbers, and rounding errors occur when we round a number to certain significant figures. In the implementation of the GDF in this paper, truncation errors do not occur, but rounding errors do. Figure 3-8 helps explain how this happens. The flowchart has been simplified to show only two major blocks-that of PSPICE and program Delta Lambda.

The cause of rounding errors is the data conversion (indicated by the broken line) in which real numbers are converted into strings

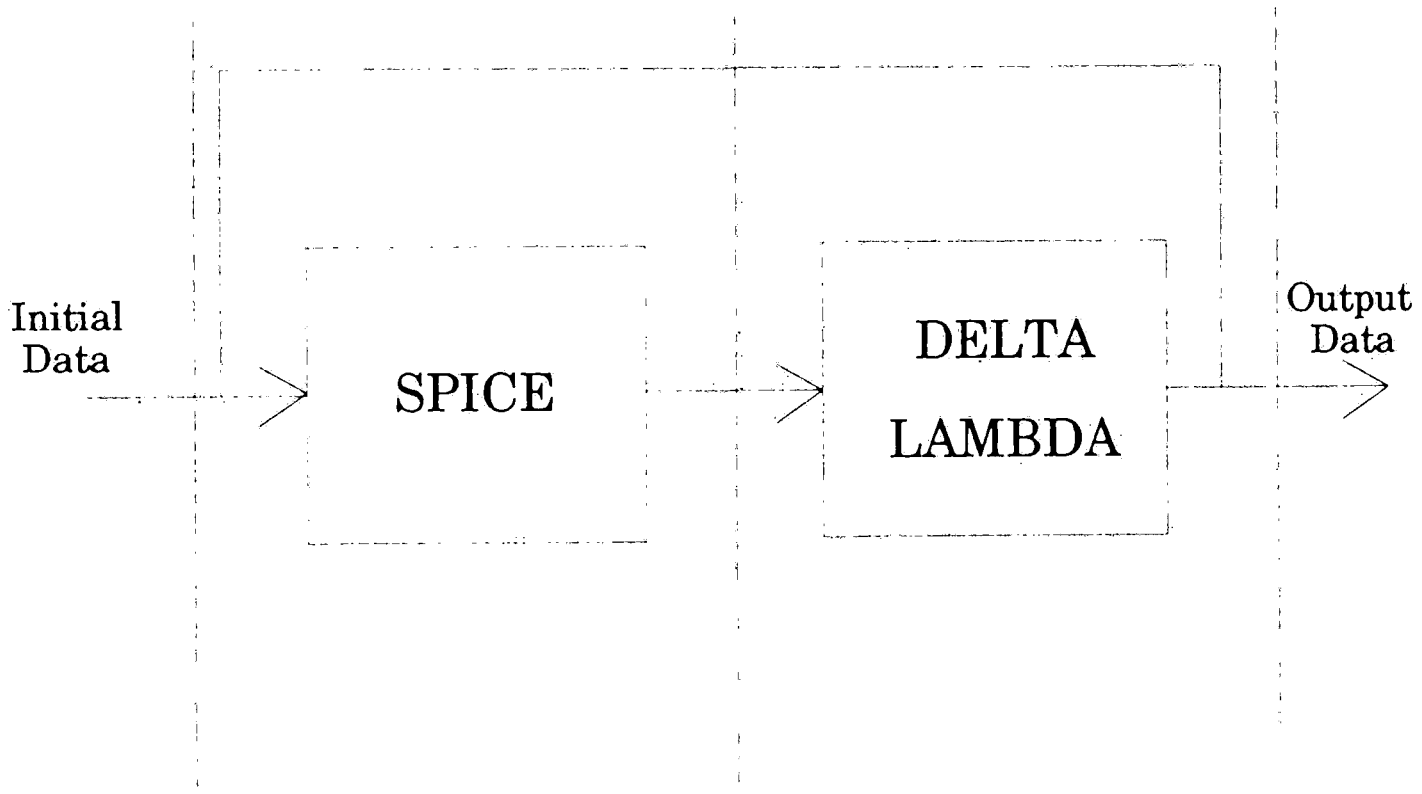

Figure 3-8: Data conversion between SPICE and Delta Lambda.

for output in a text file, and is perhaps the disadvantage of the GDF method. The first situation where this happens is when PSPICE writes it's output to it's data file where it is rounded to a floating point of four significant digits(an example is shown in the software documentation). This data is then read by program Delta Lambda and used for computation. The second time rounding occurs is when program Delta Lambda outputs it's data file composed of new values for λ, and F_y in a four significant floating point format consistent with PSPICE, where λ is read into the PSPICE input card, while F_y is read back by Delta Lambda in the next iteration. The values for $\bar{x}$ are also written in the output file but are never inputed back into either program. The rounding errors can be minimized by increasing the precision of the output of both programs. The accuracy of x is therefore limited by the precision of the output PSPICE and Delta Lambda.

The common mathematical expression for precision errors is

$$relative\ error = \frac{error}{true\ value}$$

Using the normal ouput of PSPICE which is four significant figures, the relative error would be in the order of 10^{-4} or 0.01%. Therefore if the algorithm converges, the correct expression for the value we have obtained is $x \pm 0.01\%$. The value of e displayed in the tabulated results was computed using (2.11), and even though this sometimes gets to very small values, the accuracy of x still remains in the order of 10^{-4}.

In the next chapter, the results are shown for the two groups of

nonlinearities used in this study, those which generate even harmonics and those which generate odd harmonics. The use of a weighting function to improve convergence is discussed, and the results are also given.

Chapter 4
Results of Numerical Studies

The objective of the experiments made in this study was to test the performance of the GDF under the following criteria: Convergence using only the fundamental frequency in the computation; Convergence when multiple frequencies are used; and it's relative accuracy compared to the results of a SPICE transient analysis. The results of the transient analysis feature of SPICE, which is a time domain analysis, provides an excellent comparison for the frequency domain based GDF algorithm. Therefore, the types of circuits chosen were those that can be equivalently modeled in SPICE. The data gathered using only the fundamental harmonic show how the GDF performed under different sizes of input voltage, and those for multiple frequencies show how it performed under two types and two levels of harmonic distortion. Two multiple frequency generating circuits were used: one which generates significant odd harmonics, and one which generates significant even harmonics. The input to the circuits were varied in order to test the convergence under two conditions: when the total harmonic distortion is "small", that is when it is less than 3%; and when the total harmonic distortion is "large", which is categorized as above 3%, but in these experiments, typically between 10 – 12%. The results showing the use of weighting functions to improve convergence is shown at the end of this chapter.

4.1 Types of Circuits Studied

The topology of the circuits used in the experiments is basically composed of a capacitor and a nonlinear device characterized by a polynomial, and is shown in Figure 4-1a. This circuit is flexible enough to be used to evaluate the different criteria we have set above, and can also be modeled in the SPICE transient analysis for comparison of results. The nonlinear element is broken down into it's linear and nonlinear component as shown in Figure 4-2b, where we have let $g_0 = 1$ and $g_1 = 1$ for simplicity. A saturating nonlinearity, where $n = 1/3$ was used in the single harmonic experiments. The saturation prevents the nonlinear element from going to unreasonably high values when large voltages were applied. This nonlinearity was also used in generating odd harmonics for multiple frequency experiments. To generate even numbered harmonics, we set $n = 2$, which generally characterizes a frequency doubler circuit, although in this case the input was carefully chosen to keep the value of the nonlinearity at a reasonable level. When the capacitor was set to $1F$, with the fundamental frequency at $1Hz$, small harmonics were produced. In order to produce large harmonic distortion, isolation was increased by letting the value of the capacitor be equal to $0.1F$, while the excitation was varied to get the desired size of distortion.

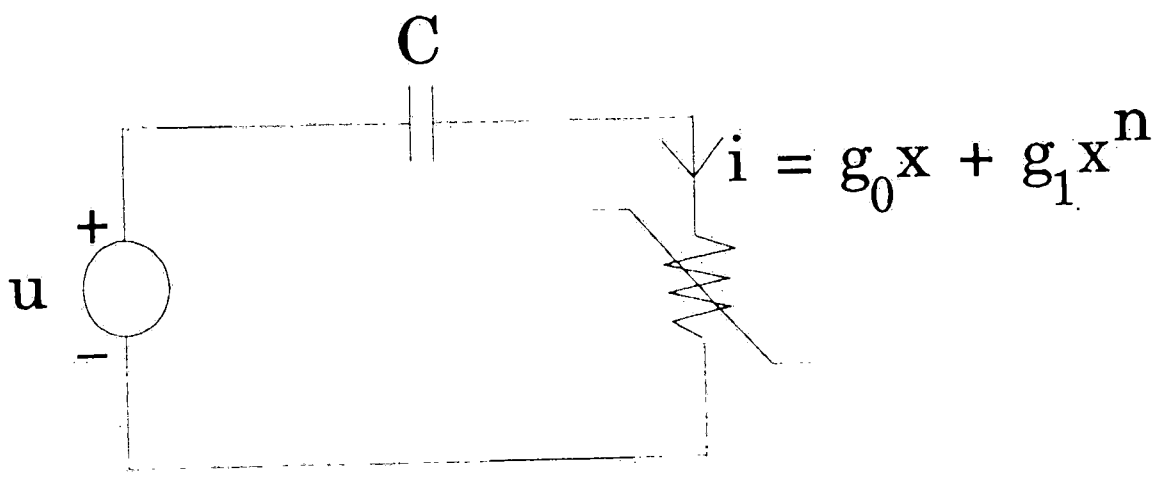

(a)

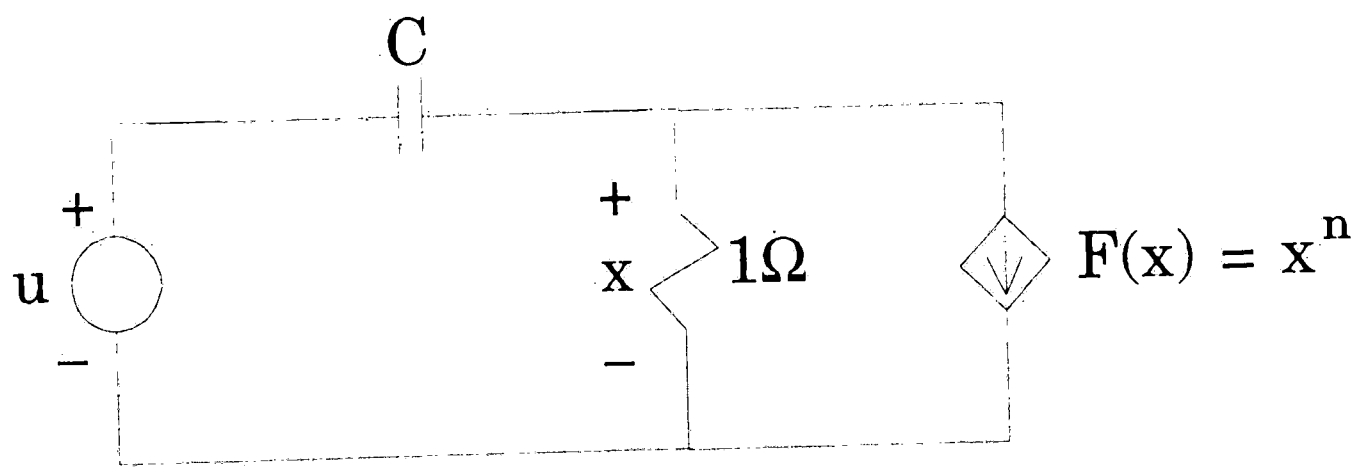

(b)

Figure 4-1: Topology of the circuits used.

4.2 Use of SPICE Transient Analysis for Comparison

It is possible to calculate the Fourier coefficients of a given signal using the transient analysis feature of SPICE. Only part of the transient waveform is used for the harmonic decomposition. The period of time used is the inverse of the fundamental frequency specified. In these experiments, the transient simulation was run for 10 periods and the segment of the waveform that was used was the last period. The % total harmonic distortion is also computed. Polynomial nonlinearities can be modeled in SPICE using a polynomial controlled source. The equivalent of the $n = 1/3$ nonlinearity is shown in Figure 4-2a, where the nonlinearity is modeled by the element *H* which is a polynomial current controlled voltage source. The independent source *Vd* is a dummy voltage and is used just to satisfy the SPICE syntax. The equivalent of the $n = 2$ nonlinearity is shown in Figure 4-2b, where the nonlinearity is modeled by the element *G*, which is a polynomial voltage-controlled current source. The result of the simulation of these circuits are shown together with the GDF results on the tables and plots to be discussed in the next section.

4.3 Convergence of the GDF

In this section, the results of the experiments that were carried out to test the performance of the GDF based on the criteria set above is presented. The numerical results are tabulated in the Appendix, where the specifications are given on the page preceding

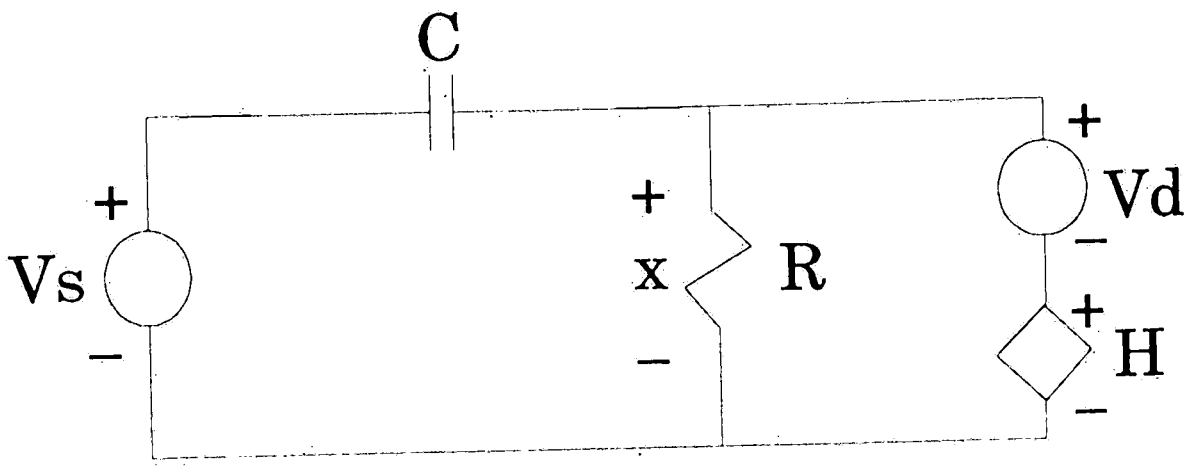

(a)

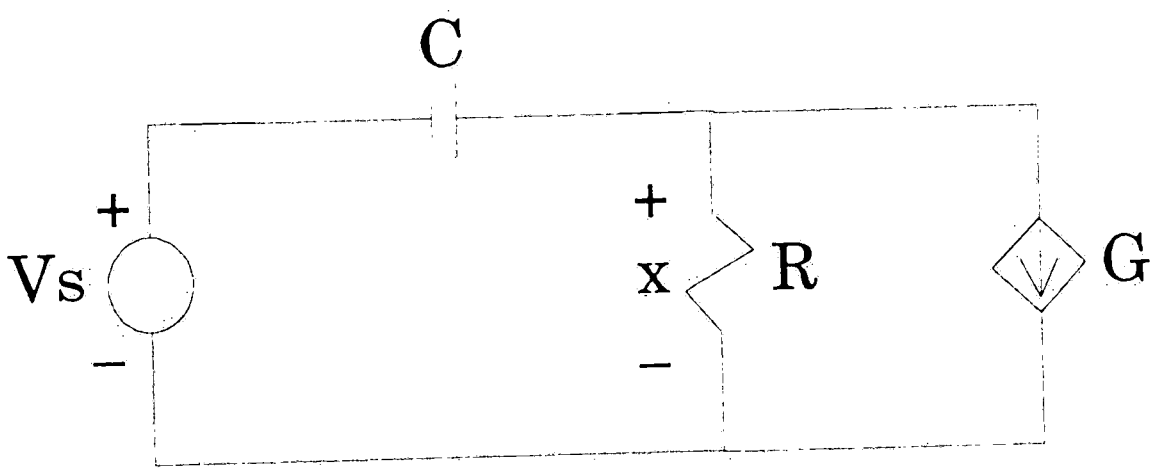

(b)

Figure 4-2: Equivalent models for SPICE transient analysis.

each table. A comparison of the results of the GDF, and that of the SPICE transient analysis is also given. The convergence of λ is compared for the different circuits studied for each criteria and are plotted on a semi-logarithmic scale. In order to compare the rate of convergence, the values of λ plotted are the normalized equivalents and were computed as follows:

$$normalized \quad \lambda = \left| \frac{\lambda^j - \lambda^f}{\Delta\lambda} \right|$$

where λ^j is the value of λ in the current iteration, λ^f is the final value when λ converges, and $\Delta\lambda$ is the total change in λ from its initial value to its final value. This means that the normalized λ initially starts at unity, and the faster it appoaches zero on each iteration step, the faster it converges. The measure of convergence is the value of the error e for the fundamental and the other significant harmonics, and both should be in the order of 10^{-5} for the circuit to be classified as having converged. A factor of 10^{-5} has also been added to the value of the normalized λ in order to set the lower limit at this number so that it can be plotted in the semi-logarithmic scale. Note that this factor is below the accuracy of computation for our experiments, as was discussed in the preceding chapter; hence, this is the reason why it is used. The relative accuracy of the GDF compared to the result of the SPICE transient analysis is also plotted in the semi-logarithmic scale, and this is based on values given in the Appendix. It should be specifically mentioned that the results of the higher harmonics of the GDF is out of phase with that

of the SPICE transient analysis, and the reason for this is just the difference in convention used by the two methods in doing the Fourier analysis. The SPICE transient analysis uses the sine function for the time domain representation of the signals in it's computation-*i.e.*, $Vsin(\omega t+\pi)$-while the GDF on the other hand uses the more standard cosine function. The fundamental, though, should be in phase.

4.3.1 Fundamental Harmonic

The order of the nonlinearity that was used for this experiment is $n = 1/3$, and the reason for this choice has been given above. The experiment was done for three different values of the input voltage u, and the results are shown in Table A-1. The convergence of λ is plotted in Figure 4-3, and is generally very fast for the three sizes of input, taking only 6 or less iterations. The comparison with the SPICE transient analysis for the output voltages, given in Figure 4-4, shows good accuracy for the the significant harmonics.

4.3.2 Small Harmonic Distortion

The first three experiments that were done here, was to repeat the three experiments of the first subsection-that is, using the same three input voltages-except this time instead of using only the fundamental, we use five harmonics in order to find out if adding harmonics to the computation would change the rate of convergence. The results are shown in Tables A-2, A-3, and A-4. The plot given in Figure 4-5 showing the convergence of λ, shows no significant

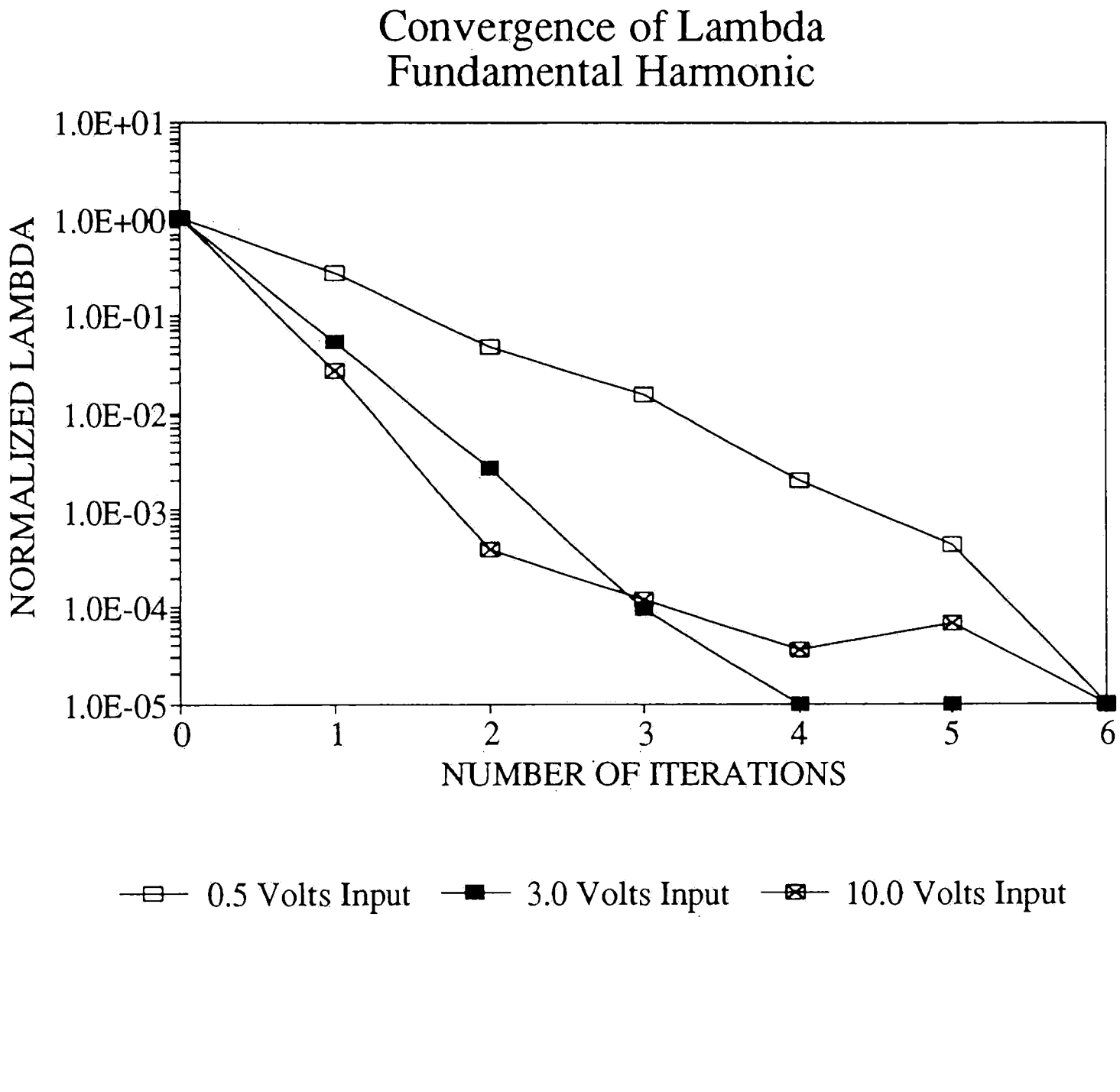

Figure 4-3: Comparison for three sizes of input voltages.

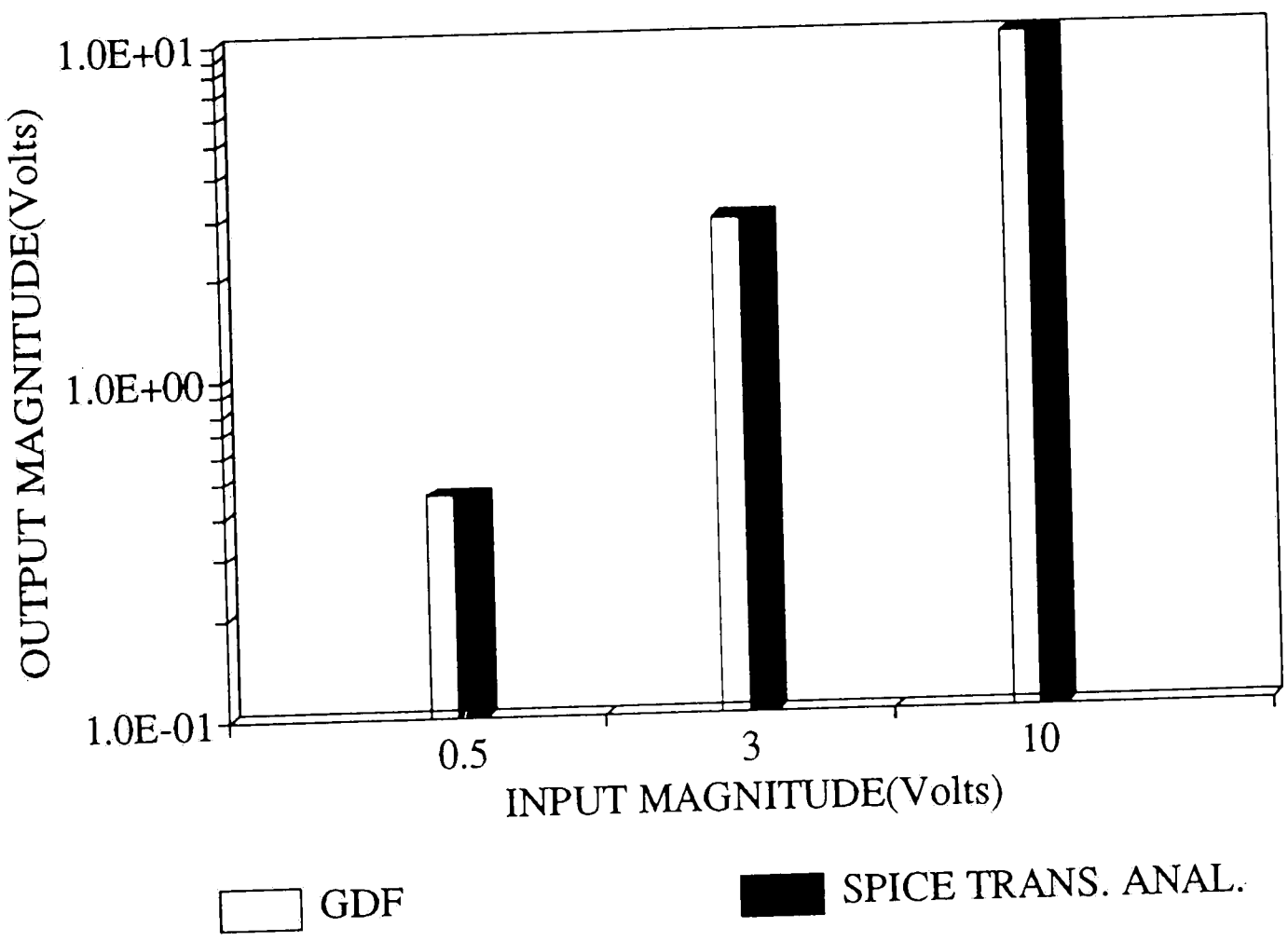

Figure 4-4: The output voltages for three sizes of input.

difference from the plot in Figure 4-3. The SPICE comparison of the output voltage for the input of $u = 3.0$, given in Figure 4-6, also shows good agreement in the significant harmonics. Note that the harmonic distortion for each of these experiments is less than 3% and is classified as "small".

The next experiment tests the circuit that produces even harmonic. The exponent of the nonlinearity in this circuit is $n = 2$, and its topology has been discussed above. The result given Table A-5, shows it converges in 9 iterations which is still relatively fast, and the plot in Figure 4-7, also shows good agreement with SPICE for the significant harmonics.

4.3.3 Large Harmonic Distortion

As discussed above, the harmonic distortion can be enlarged with increased isolation of the nonlinear element, specifically for our circuit, by decreasing the capacitance by an order of magnitude. The input voltages of 3.0, and 0.6 for the odd and even harmonics respectively, produced desired distortion which fits our description of "large". The odd harmonic result is given in Table A-6, and it shows that the errors of the significant harmonics did not go down to the order of 10^{-5} which is our gauge for convergence. The algorithm in this case remained stable, although it was not driving the value of the errors down either, so the iteration was stopped. The number of frequencies were decreased to three, to find out if the convergence would improve, and it did drive the error of the fundamental down as shown in Table A-7, but the 3rd harmonic error remained an order of

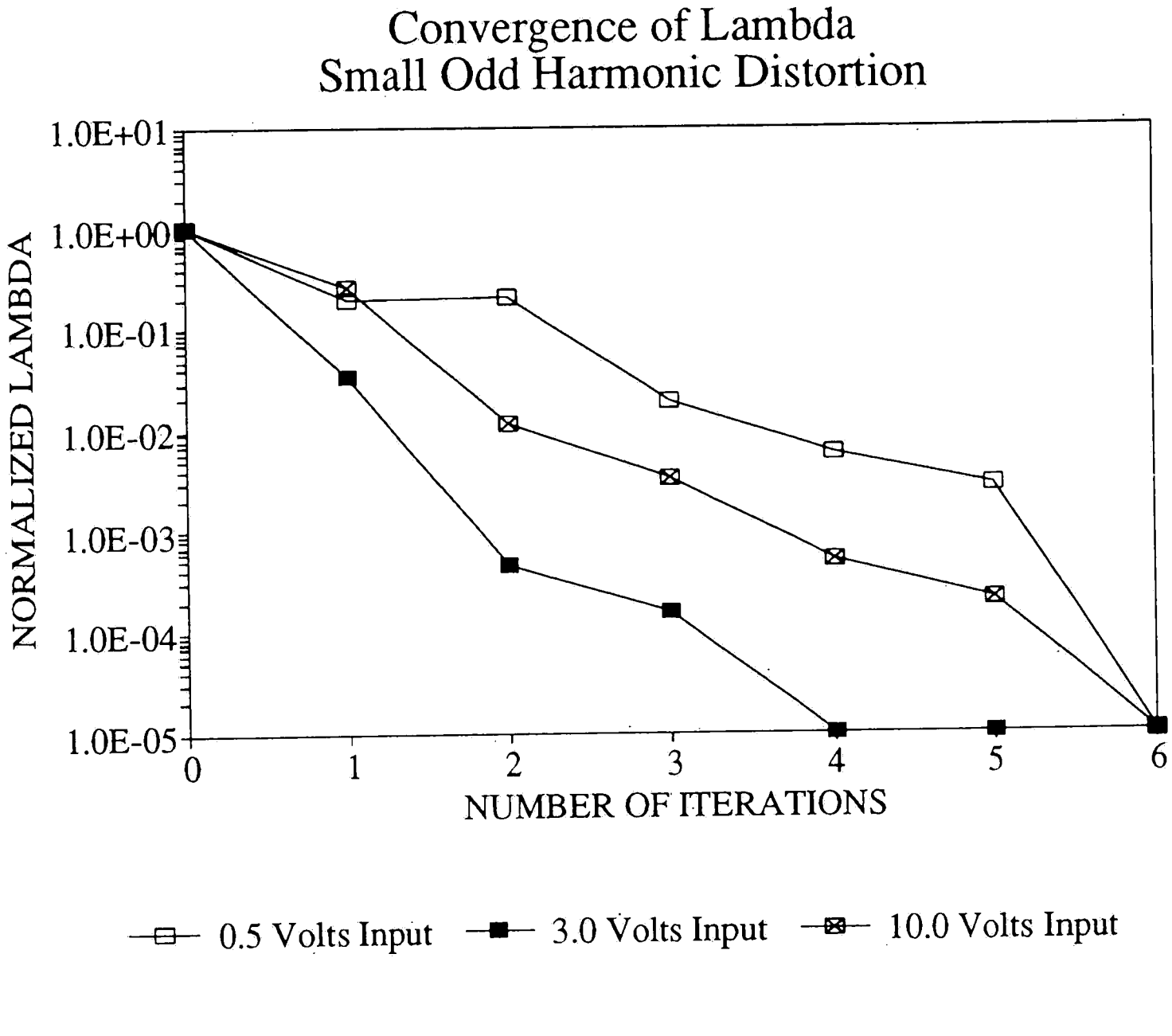

Figure 4-5: Multiple frequency results for three sizes of input.

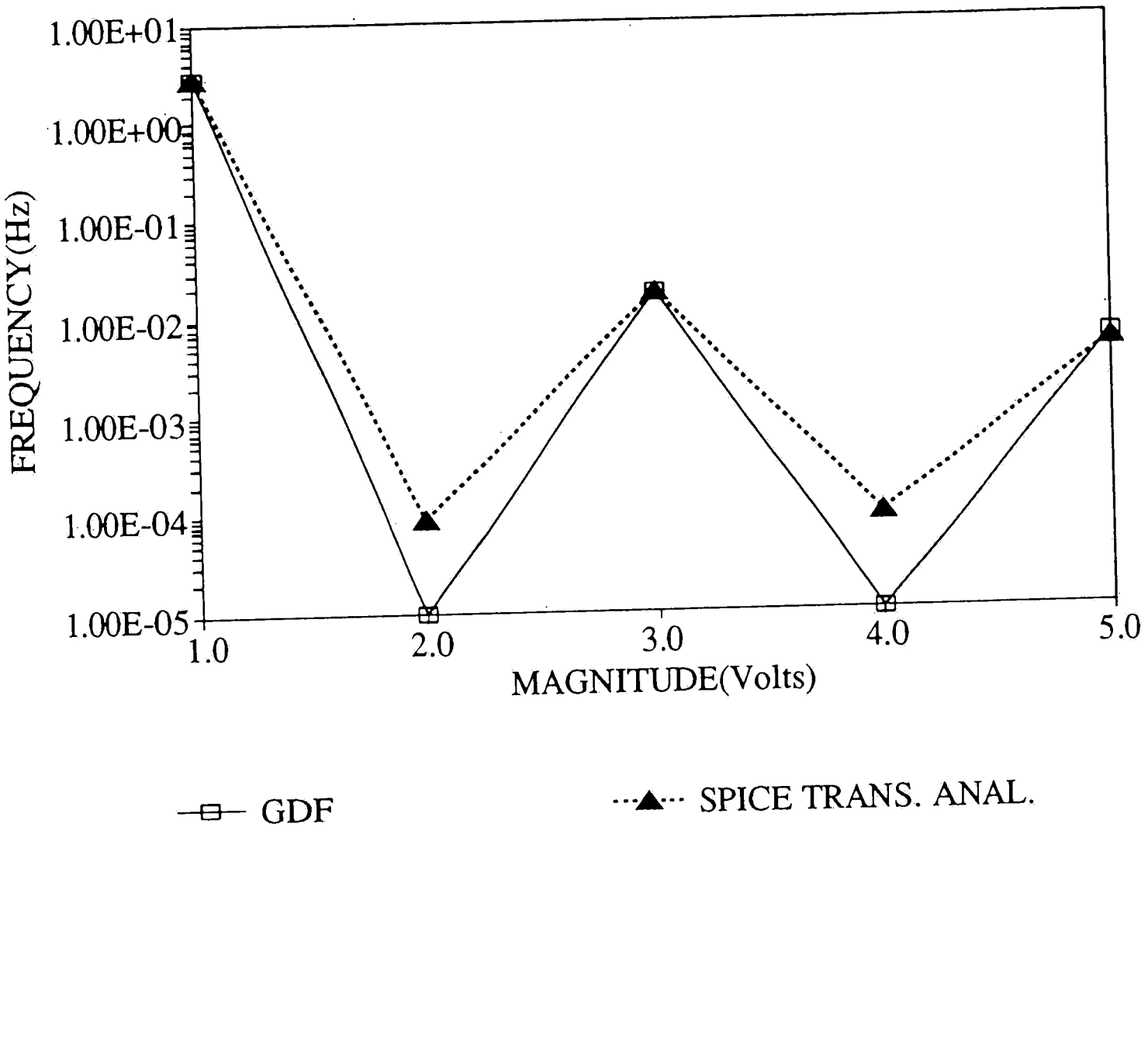

Figure 4-6: The output voltage for small distortion, odd harmonic.

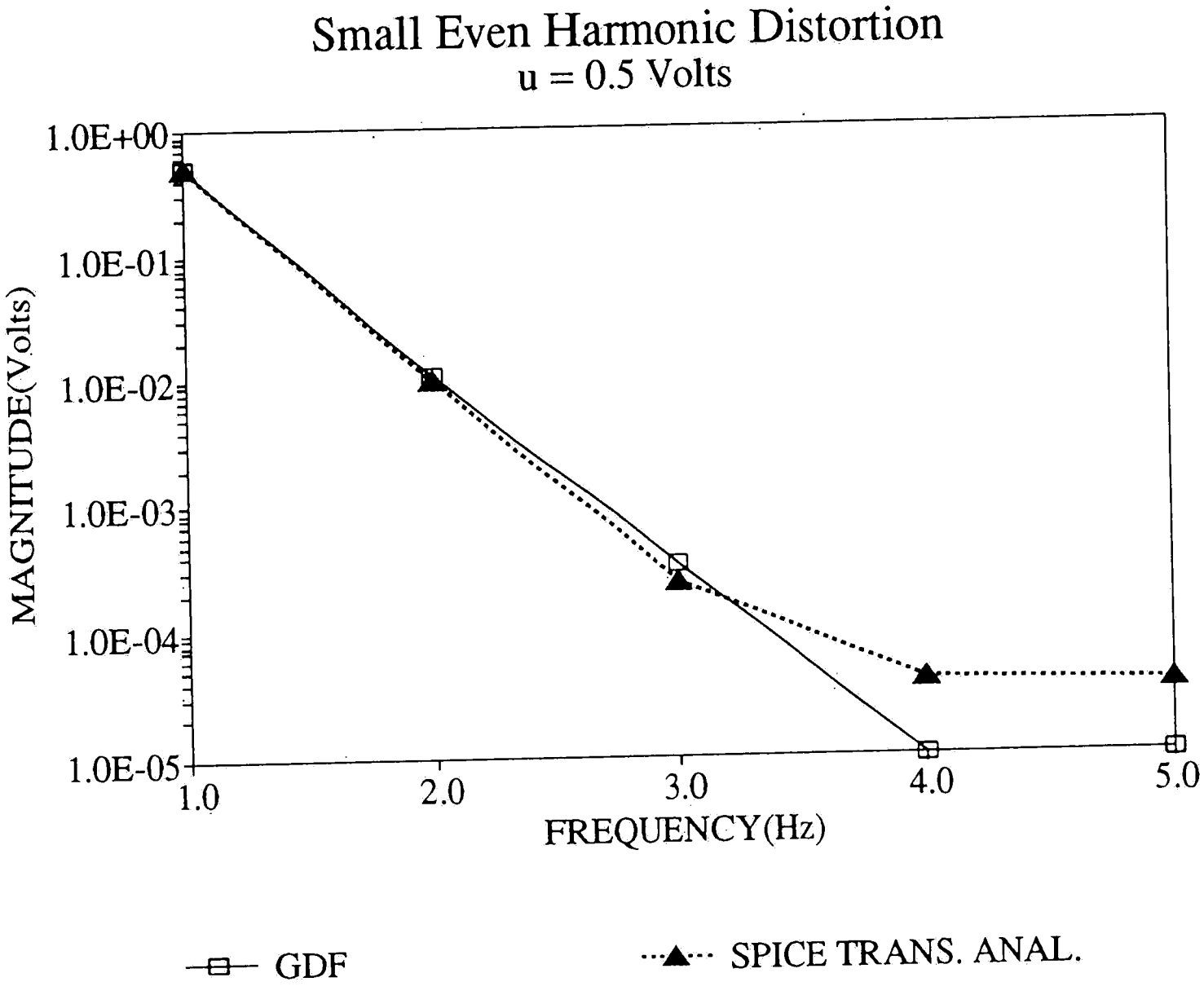

Figure 4-7: The output voltage for small distortion, even harmonic.

magnitude above the standard. The iteration was also stopped in this case because it was again not driving the errors down any farther. However, when only one harmonic was used, convergence was attained in 16 iterations as shown in Table A-8.

It was also slow in the even harmonic case, but it did converge in 23 iterations. Figure 4-8 shows the comparison with SPICE for this case, and there is a close match in the fundamental, but the difference becomes more sizable for higher harmonics.

The rate of convergence of the four categories are plotted together in Figure 4-9. This shows that the algorithm is slowed down by larger harmonic distortions. The large even harmonic case actually starts slower than the large odd case, but unlike the odd case, it eventually converges.

4.4 Use of Weighting Function to Improve Convergence

In this section, experiments are carried out to attain convergence for the large odd harmonic case, by the use of a weighting function to operate on the error, first derivative of the error, and second derivative of the error. Weights are introduced into the numerical computation to make the accuracy better for one part of the data than another, and provided they are positive, they do not affect the methods or theory of approximation [16]. Any vector can be used as the weight-for example $(1, 0, 1, 0, 1)^T$. Tables A-10, A-11, and A-12 show the best combinations of weights that were able

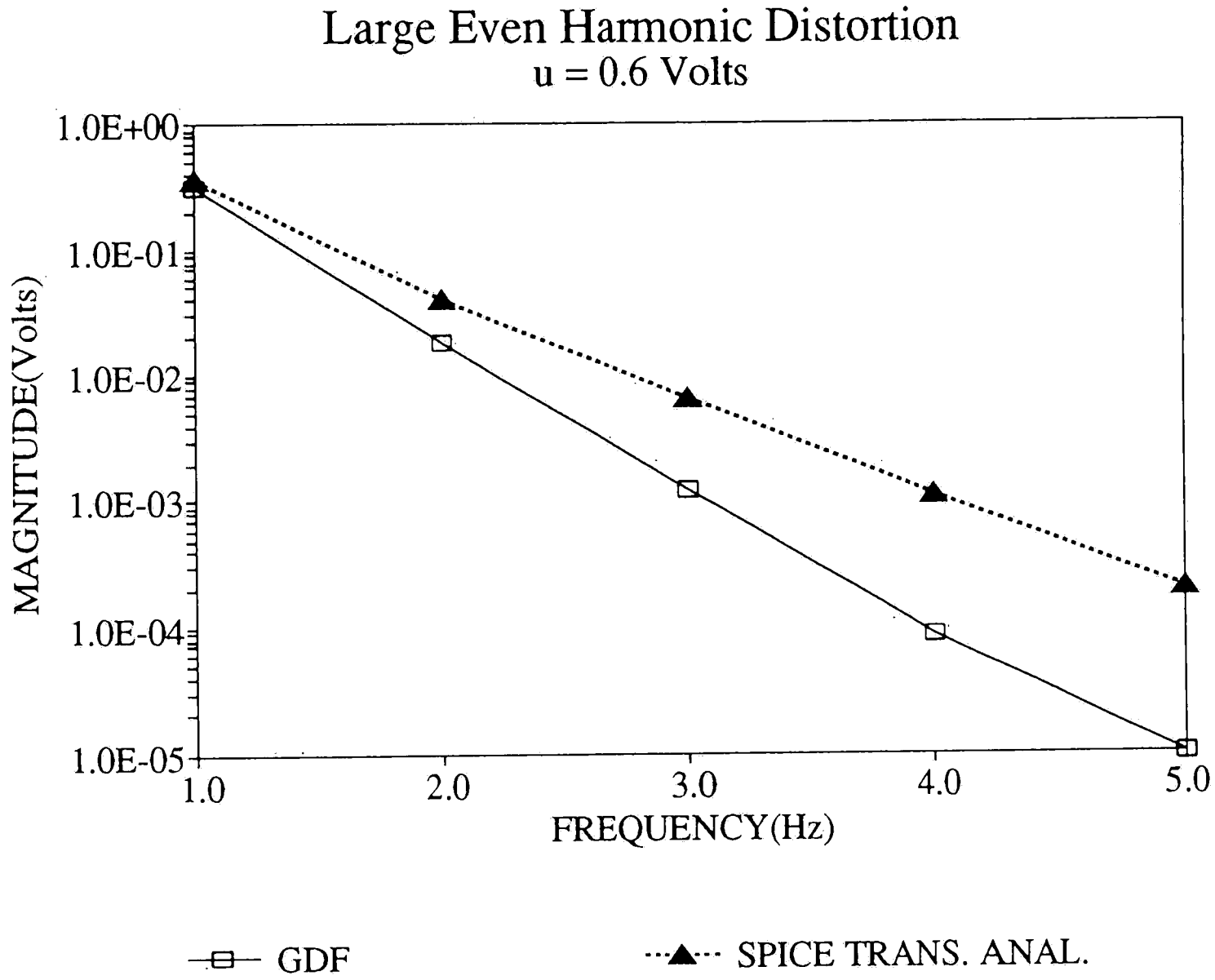

Figure 4-8: The output voltage for large distortion, even harmonic.

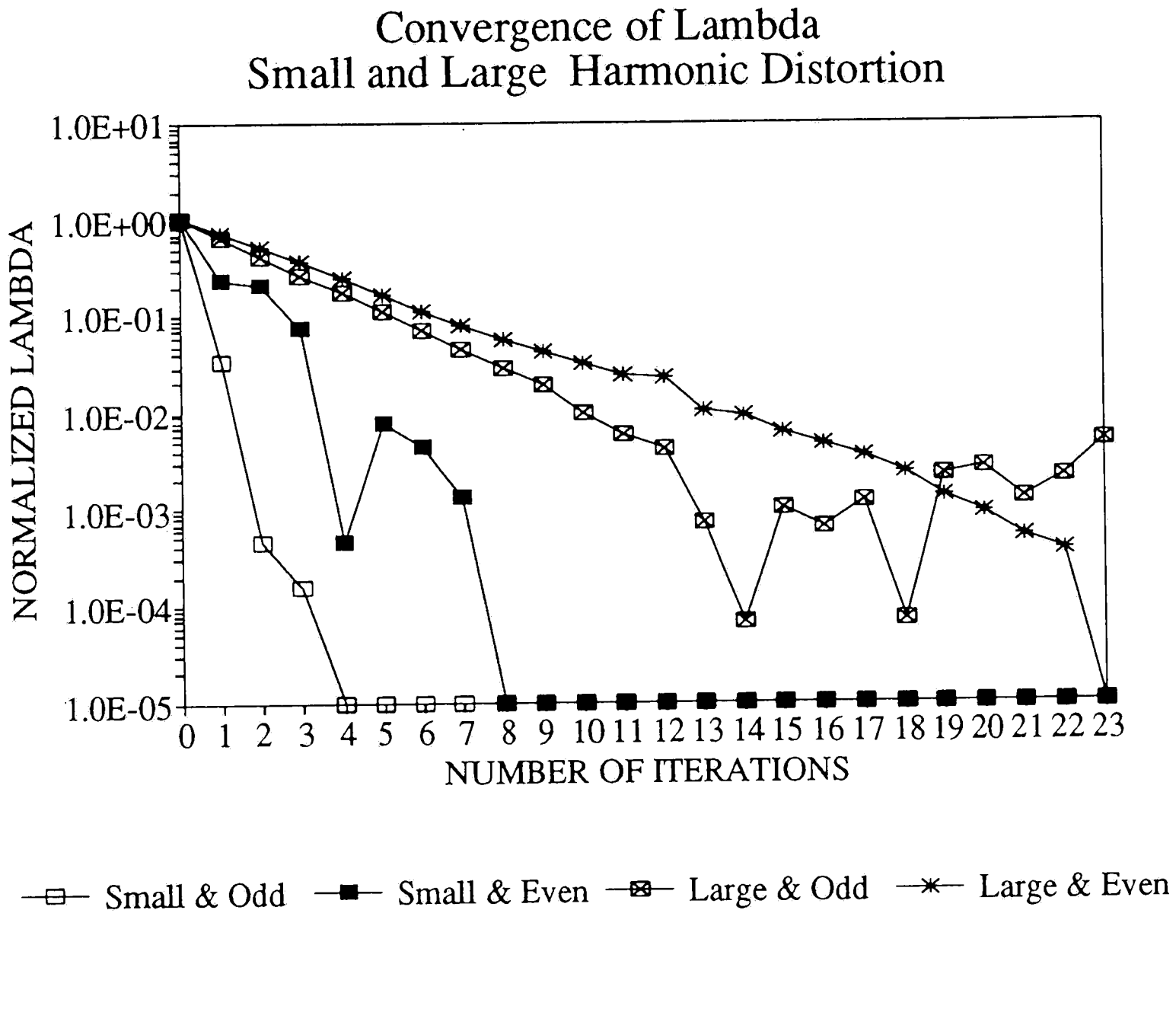

Figure 4-9: Comparison for different sizes and types of distortion.

to attain convergence for the large odd harmonic distortion. The weight that was used for each is given in the specifications. The weights used for Table A-12 requires special mention, they are the normalized value of the first three harmonics, while the other two harmonics were given zero values. The elements of the weight vector for Table A-12 were computed as follows:

$$x_n' = \frac{x_n}{norm(x)} \quad for \quad n = 1,2,3$$

where $norm(x)$ is the norm of the output vector x and is given by

$$norm(x) = \sqrt{x_1^2 + x_2^2 + x_3^2}$$

The computation for the transform in this case used only the first three harmonic coefficients because the the values of the transform are used only for the computations of the error vector, and the two higher harmonics of the error are neglected anyway. It is the results from Table A-12 that was used for in plots in Figures 4-10 and 4-11. Figure 4-10 shows a significant improvement in the convergence of lambda when a weighting function is used, and there is also a good match with the SPICE transient analysis results in Figure 4-11. When the normalized weights were tried on the large even harmonic case, the rate of convergence also improved. The result of this is given in Table A-13. It shows that it converged in only 16 iterations, compared to 23 when no weights were applied.

The results of the last two experiments are given in Tables A-14 and A-15. These circuits are the fast converging small harmonic distortion type, and when the weighting function was

applied on them, the results showed no diversion from previous values obtained. The results from Table A-3 and A-14 are also plotted in Figure 4-10, and show no significant difference from each other. The weighting function as applied in these experiments shows that it can improve on slowly converging circuits, while it produces similar results for already fast converging circuits.

The implications of the data gathered in these experiments are discussed in the conclusion.

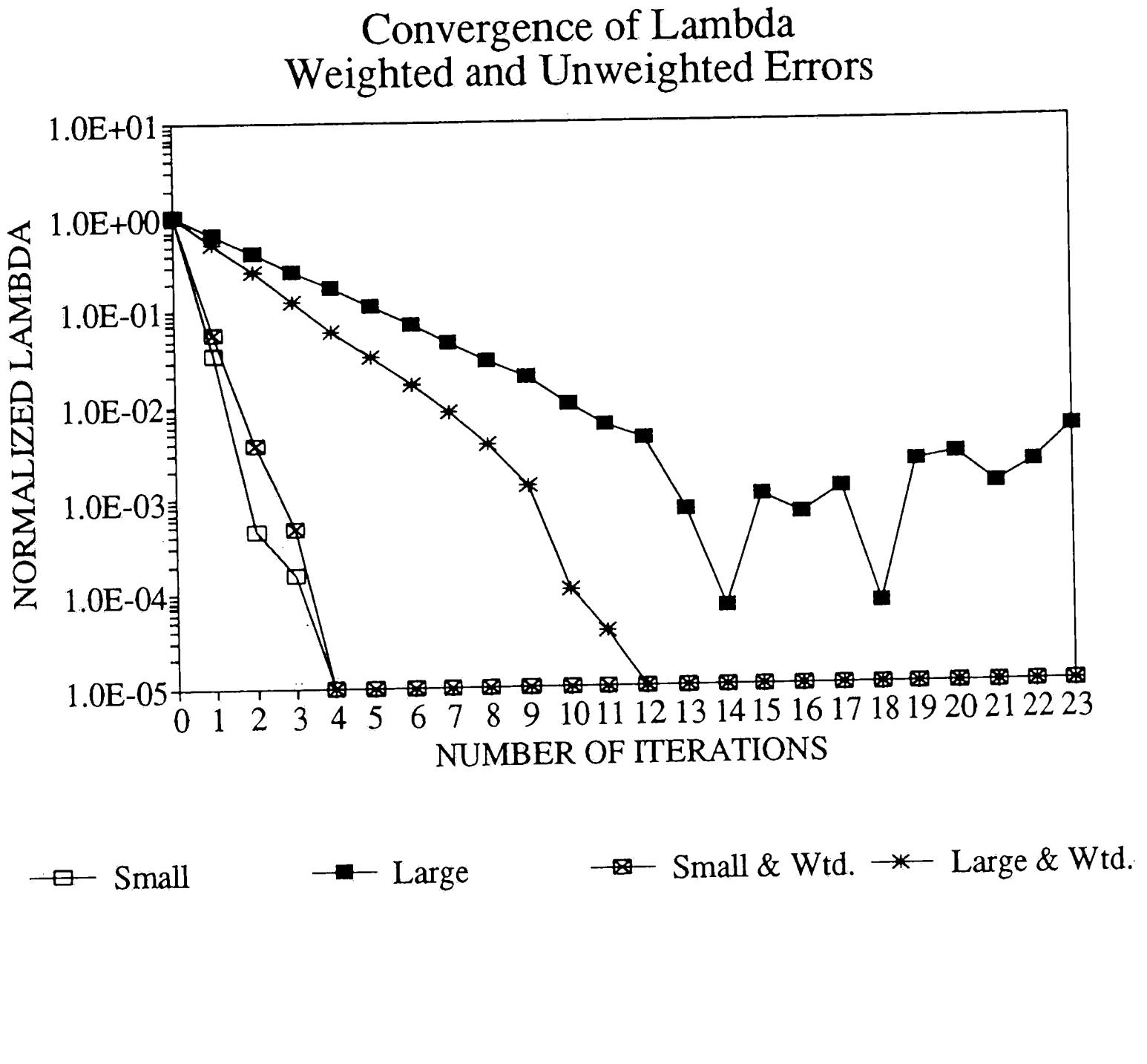

Figure 4-10: The effect of weights on the odd harmonic cases.

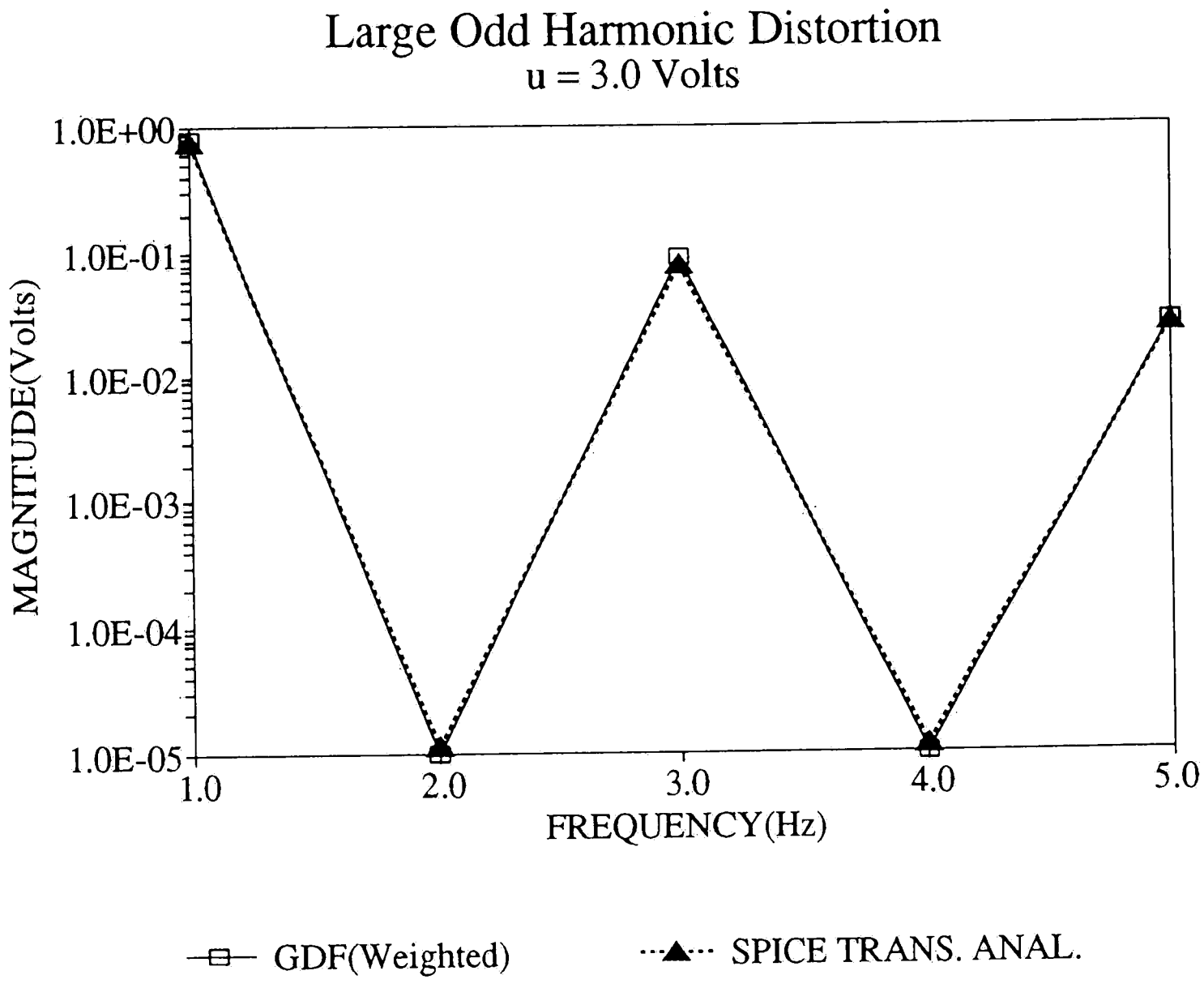

Figure 4-11: The output voltage when weights were applied.

Conclusions

The GDF showed exceptional convergence for different sizes of input voltage using the fundamental frequency, and this was also true for multiple frequencies with small harmonic distortion. When the harmonic distortion was increased, however, the convergence slowed down, especially in the odd harmonic case. This problem was corrected with the use of weighting functions to operate on the error vectors, and resulted in a considerable improvement of convergence. The results of the output voltages of the GDF generally agreed with that of the SPICE transient analysis for both the single frequency and multiple frequency cases.

One attempt to explain the deceleration of convergence when the harmonic distortion is increased is that too many variables are being optimized, and this is also a general problem of the harmonic balance method. Weighting the errors magnifies the more important data to be optimized, and diminishes the less important ones. This explains the improvement of convergence when the weighting function is used. Weighting does not have a significant effect on the accuracy of the output voltages, nor does it affect the rate of fast converging circuits, as shown in the results. Weighting should therefore be used on circuits where the algorithm is stable, but is slowly converging.

An interesting result of this work shows the good agreement of the GDF and the SPICE transient analysis results on the significant

harmonics, while it can be observed that the GDF has generally lower values for the insignificant harmonics. The reason for this is that SPICE is interpolating between two points, in order to get the value for a particular harmonic; hence, accurracy is dependent on the number of time points used in the transient analysis. The accurracy is improved if more time points are used, but this would also lengthen the computation time. This is a general problem of time domain based algorithms, and does not happen in the frequency domain solution, and hence helps prove the frequency domain solution's suitability for periodic steady-state analysis.

Perhaps the main problem the GDF algorithm has when it is implemented using SPICE, is from the user point of view. The computational speed is dependent on the execution speed of the SPICE program. Using the professional PSPICE version 3.07 on the 80386 microcomputer, the SPICE AC analysis timed an average of 2.7 seconds for each run, and it is executed twice for each iteration. This excludes the overhead time used by the PSPICE program (depending on how the directory is formatted) to do it's file swapping. The rest of the algorithm took around 5 seconds to execute. However, with the fast rate of convergence that was experienced in this study, the GDF would still be more economical than a time domain based solution for long transient conditions.

The goal of this paper was to introduce the GDF, and to show that the algorithm yields good convergence. Both goals have been met, and the next step for a future researcher would be to test the

applicability of the algorithm to different types of nonlinearity, and to make possible improvements if it shows weaknesses when applied to some types. An obvious choice of a circuit is the one that involves an exponential nonlinearity. This type of nonlinearity can also be modeled in the SPICE transient analysis for comparison. Another route to take would be the extension of the algorithm to do a harmonic balance solution. The equations have been formulated in chapter 2, and all the researcher has to to is to extend the software that has been implemented to include this type of analysis.

References

1. T. J. Aprille and T. N. Trick, "Steady-state analysis of nonlinear circuits with periodic input", *Proc. IEEE*, Vol. 60, 1972, pp. 108-114.

2. S. Skelboe, "Computation of the periodic steady-state response of nonlinear networks by extrapolation method", *IEEE Trans. Circuits and Systems*, Vol. CAS-27, 1980, pp. 161-175.

3. R. J. Kochenburger, "A frequency response method for analyzing and synthesizing contactor servomechanism", *Trans. AIEE*, Vol. 69, 1950, pp. 270-283.

4. M. S. Nakhla and J. Vlach, "A piecewise harmonic balance technique for the determination of periodic response of nonlinear sytems", *IEEE Trans. Circuits and Systems*, Vol. CAS-23, 1976, pp. 85-91.

5. K. Gopal, M. S. Nahkla, K. Singhal, and J. Vlach, "Distortion analysis of transistor networks", *IEEE Trans. Circuits and Systems*, Vol. CAS-25, 1978, pp. 99-106.

6. F. Filicori, V. A. Monaco, and C. Naldi, "Simulation and design of microwave class-C amplifiers through harmonic analysis", *IEEE Trans. Microwave Theory and Techniques*, Vol. MTT-27, 1979, pp. 1043-1051.

7. R. J. Hicks, and P. J. Khan, "Numerical analysis of subharminic mixers using accurate and approximate models", *IEEE Trans. Microwave Theory and Techniques*, Vol. MTT-30, 1979, pp. 2113-2120.

8. A. Gelb and W. E. Vander Velde, *Multiple-input describing functions and nonlinear system design,* McGraw-Hill, New York, 1968.

9. R. Sridhar, "A general method for deriving the describing functions for a certain class of nonlinearities", *IRE Trans. Automatic Control*, Vol. AC-5, 1960, pp. 135-141.

10. L. O. Chua and P. M. Lin, *Computer-aided analysis of electronic circuits: algorithms & computational techniques,* McGraw-Hill, New York, 1975.

11. K. S. Kundert and A. Sangiovanni-Vincentelli, "Simulation of nonlinear circuits in the frequency domain", *IEEE Trans. Computer-Aided Design*, Vol. CAD-5, 1986, pp. 521-535.

12. D. R. Frey, "A simple generalized modeling technique for nonlinear networks", *Proc. IEEE Int'l. Symp. Circuits and Systems*, Vol. 1, 1984, pp. 343-347.

13. L. W. Nagel, "SPICE: a computer program to simulate semiconductor circuits", Tech. report Memo No. ERL-M520, University of California, Berkeley, May 1975.

14. W. Blume, "Computer circuit simulation", *BYTE*, Vol. 11-7, 1986, pp. 165.

15. P. W. Tuinenga, *SPICE: A guide to circuit simulation and analysis using PSpice,* Printice-Hall, Englewood Cliffs, New Jersey, 1988.

16. J. R. Rice, *Numerical methods, software, and analysis,* McGraw-Hill, New York, 1983.

Appendix A

SPECIFICATIONS FOR TABLE A-1

Circuit:	See Figure 4-1
Nonlinearity:	$F(x)^{1/3}$
Capacitance(C):	1.0F
Initial λ:	1.000E+00 + j0.000E+00
Final λ(u=0.5V):	1.853E+00 - j1.027E+00
No. of Iterations(u=0.5V):	6
Final λ(u=3.0V):	7.815E-01 - j1.422E-01
No. of Iterations(u=3.0V):	4
Final λ(u=10.0V):	3.200E-01 - j1.194E-01
No. of Iterations(u=10.0V):	6

COMPARISON OF SPICE TRANSIENT ANALYSIS AND THE GDF OUTPUT VOLTAGES

SPICE:

Input Voltage	Fourier Comp	Phase (DEG)
5.000E-01	4.500E-01	2.520E+01
3.000E+00	2.908E+00	1.401E+01
1.000E+01	9.802E+00	1.127E+01

GDF: (from Table A-1)

Freq (HZ)	Fourier Comp	Phase (DEG)
5.000E-01	4.522E-01	2.530E+01
3.000E+00	2.911E+00	1.402E+01
1.000E+01	9.806E+00	1.128E+01

Input V	Initial F_y	Final Voltage (x)	Final F_y
5.000E-01	-5.000E-01 - j5.000E-01	4.088E-01 + j1.932E-01	-1.509E-01 + j4.416E-01
3.000E+00	-5.000E-01 - j5.000E-01	2.824E+00 + j7.053E-01	-7.006E-01 + j2.498E+00
1.000E+01	-5.000E-01 - j5.000E-01	9.617E+00 + j1.918E+00	-1.011E+00 + j1.714E+00
Input V	Errors	First Derivative	Second Derivative
5.000E-01	3.176E-05 + j3.151E-05	6.101E-02 - j4.468E-02	3.399E-03 + j2.507E-02
3.000E+00	-2.180E-05 - j1.252E-05	2.290E-01 - j3.935E-01	9.824E-02 + j1.031E-01
1.000E+01	-5.474E-05 - j5.256E-05	6.276E-01 - j1.443E+00	4.098E-01 + j2.949E-01

Table A-1: The use of only the fundamental harmonic.

SPECIFICATIONS FOR TABLE A-2

Circuit:	See Figure 4-1
Nonlinearity:	$F(x)^{1/3}$
Voltage Source(u):	$0.5\cos(2\pi)t$
Capacitance(C):	1.0F
Initial λ:	1.000E+00 + j0.000E+00
Final λ:	3.349E+00 + j2.785E-01
Number of Iterations:	6

COMPARISON OF SPICE TRANSIENT ANALYSIS AND THE GDF OUTPUT VOLTAGES

SPICE:

Freq (HZ)	Fourier Comp	Phase (DEG)
1.000E+00	4.500E-01	2.520E+01
2.000E+00	1.074E-06	9.001E+01
3.000E+00	9.323E-03	1.752E+02
4.000E+00	1.072E-06	8.997E+01
5.000E+00	2.776E-03	-1.319E+02

% Total harmonic distortion: 2.185E+00

GDF: (from Table A-2)

Freq (HZ)	Fourier Comp	Phase (DEG)
1.000E+00	4.511E-01	2.522E+01
2.000E+00	3.174E-07	-7.928E+01
3.000E+00	9.153E-03	-7.130E+00
4.000E+00	5.417E-08	-1.663E+01
5.000E+00	2.741E-03	-1.389E+02

Freq	Initial F_y	Final Voltage (x)	Final F_y
1.000E+00	-5.000E-01 - j5.000E-01	4.081E-01 + j1.922E-01	-5.125E-01 - j3.173E-01
2.000E+00	-5.000E-03 - j5.000E-03	5.905E-08 - j3.119E-07	-3.295E-07 + j6.970E-07
3.000E+00	-5.000E-03 - j5.000E-03	9.082E-03 - j1.136E-03	-6.180E-02 - j1.733E-01
4.000E+00	-5.000E-03 - j5.000E-03	5.190E-08 + j1.550E-08	-2.280E-07 + j1.719E-07
5.000E+00	-5.000E-03 - j5.000E-03	-2.064E-03 - j1.803E-03	-4.996E-02 + j7.530E-02
Freq	Errors	First Derivative	Second Derivative
1.000E+00	-2.076E-05 + j6.785E-05	4.899E-02 - j2.979E-02	-5.540E-04 + j1.456E-02
2.000E+00	-9.926E-08 + j2.734E-07	-2.007E-08 - j1.114E-08	2.441E-09 - j2.251E-09
3.000E+00	-2.866E-05 - j2.524E-05	4.197E+00 - j4.520E-04	4.288E-05 + j1.372E-01
4.000E+00	-5.687E-08 + j6.009E-09	-2.567E-10 - j2.019E-09	1.529E-10 + j5.729E-12
5.000E+00	7.656E-06 + j7.363E-06	-6.217E-05 + j5.649E-05	-2.783E-06 - j4.157E-06

Table A-2: Small odd harmonic distortion with input u = 0.5V.

SPECIFICATIONS FOR TABLE A-3

Circuit:	See Figure 4-1
Nonlinearity:	$F(x)^{1/3}$
Voltage Source(u):	$3.0\cos(2\pi)t$
Capacitance(C):	1.0F
Initial λ:	1.000E+00 + j0.000E+00
Final λ:	5.508E-01 - j1.838E-01
Number of Iterations:	4

COMPARISON OF SPICE TRANSIENT ANALYSIS AND THE GDF OUTPUT VOLTAGES

SPICE:

Freq (HZ)	Fourier Comp	Phase (DEG)
1.000E+00	2.908E+00	1.401E+01
2.000E+00	3.056E-05	9.079E+01
3.000E+00	1.741E-02	1.367E+02
4.000E+00	3.057E-05	9.042E+01
5.000E+00	5.160E-03	1.641E+02

% Total harmonic distortion: 6.307E-01

GDF: (from Table A-3)

Freq (HZ)	Fourier Comp	Phase (DEG)
1.000E+00	2.910E+00	1.401E+01
2.000E+00	9.184E-09	-1.080E+02
3.000E+00	1.787E-02	-4.323E+01
4.000E+00	1.379E-08	1.763E+02
5.000E+00	5.390E-03	1.636E+02

Freq	Initial F_y	Final Voltage (x)	Final F_y
1.000E+00	-5.000E-01 - j5.000E-01	2.823E+00 + j7.046E-01	-8.002E-02 + j5.378E-01
2.000E+00	-5.000E-03 - j5.000E-03	-2.832E-09 - j8.736E-09	1.563E-07 - j2.439E-07
3.000E+00	-5.000E-03 - j5.000E-03	1.302E-02 - j1.224E-02	-2.443E-01 - j2.193E-01
4.000E+00	-5.000E-03 - j5.000E-03	-1.376E-08 + j8.953E-10	-1.577E-08 - j4.876E-09
5.000E+00	-5.000E-03 - j5.000E-03	-5.170E-03 + j1.523E-03	5.170E-03 + j1.554E-01
Freq	Errors	First Derivative	Second Derivative
1.000E+00	-5.082E-06 - j1.722E-05	2.191E-01 - j4.072E-01	1.083E-01 + j9.936E-02
2.000E+00	2.091E-06 + j2.387E-07	-7.359E-10 + j1.385E-10	-7.250E-12 - j1.216E-10
3.000E+00	3.629E-06 - j3.028E-06	-6.044E-04 - j7.626E-04	8.832E-05 - j5.857E-05
4.000E+00	1.616E-09 - j1.526E-09	3.298E-11 + j5.850E-11	-4.947E-12 + j2.389E-12
5.000E+00	-2.240E-06 - j3.095E-06	4.124E-05 + j1.717E-04	-1.137E-05 + j2.127E-06

Table A-3: Small odd harmonic distortion with input u = 3.0V.

SPECIFICATIONS FOR TABLE A-4

Circuit:	See Figure 4-1
Nonlinearity:	$F(x)^{1/3}$
Voltage Source(u):	$10.0\cos(2\pi)t$
Capacitance(C):	1.0F
Initial λ:	1.000E+00 + j0.000E+00
Final λ:	-4.198E-01 - j9.214E-02
Number of Iterations:	6

COMPARISON OF SPICE TRANSIENT ANALYSIS AND THE GDF OUTPUT VOLTAGES

SPICE:

Freq (HZ)	Fourier Comp	Phase (DEG)
1.000E+00	9.802E+00	1.127E+01
2.000E+00	3.964E-05	9.610E+01
3.000E+00	2.615E-02	1.279E+02
4.000E+00	3.974E-05	9.310E+01
5.000E+00	7.774E-03	1.498E+02

% Total harmonic distortion: 2.812E-01

GDF: (from Table A-4)

Freq (HZ)	Fourier Comp	Phase (DEG)
1.000E+00	9.805E+00	1.128E+01
2.000E+00	9.384E-09	2.616E+01
3.000E+00	2.654E-02	-5.217E+01
4.000E+00	1.681E-09	-1.541E+02
5.000E+00	7.957E-03	1.492E+02

Freq	Initial F_y	Final Voltage (x)	Final F_y
1.000E+00	-5.000E-01 - j5.000E-01	9.616E+00 + j1.918E+00	6.293E+00 + j2.182E+00
2.000E+00	-5.000E-03 - j5.000E-03	8.423E-09 + j4.137E-09	1.874E-07 + j1.830E-07
3.000E+00	-5.000E-03 - j5.000E-03	1.628E-02 - j2.097E-02	-3.990E-01 - j2.901E-01
4.000E+00	-5.000E-03 - j5.000E-03	-1.512E-09 - j7.347E-10	-2.812E-08 + j7.966E-08
5.000E+00	-5.000E-03 - j5.000E-03	-6.837E-03 + j4.070E-03	1.300E-01 + j2.104E-01
Freq	Errors	First Derivative	Second Derivative
1.000E+00	-3.961E-05 - j7.160E-05	4.514E-01 - j1.511E+00	4.702E-01 + j1.899E-01
2.000E+00	-2.388E-08 + j1.028E-08	3.652E-10 - j6.631E-10	1.401E-10 + j6.386E-11
3.000E+00	-2.456E-07 + j7.224E-10	-1.101E-03 - j9.107E-04	1.074E-04 - j1.154E-04
4.000E+00	-1.676E-09 - j4.755E-10	-3.109E-11 + j6.035E-11	-4.812E-12 - j2.624E-12
5.000E+00	1.464E-07 + j1.072E-06	1.273E-05 + j2.244E-04	-1.464E-05 + j7.964E-06

Table A-4: Small odd harmonic distortion with u = 10.0V.

SPECIFICATIONS FOR TABLE A-5

Circuit:	See Figure 4-1
Nonlinearity:	$F(x)^2$
Voltage Source(u):	$0.5\cos(2\pi)t$
Capacitance(C):	1.0F
Initial λ:	1.000E+00 + j0.000E+00
Final λ:	1.194E+00 - j1.409E+00
Number of Iterations:	9

COMPARISON OF SPICE TRANSIENT ANALYSIS AND THE GDF OUTPUT VOLTAGES

SPICE:

Freq (HZ)	Fourier Comp	Phase (DEG)
1.000E+00	4.959E-01	6.454E+00
2.000E+00	9.745E-03	1.616E+01
3.000E+00	2.623E-04	2.536E+01
4.000E+00	1.475E-05	4.243E+01
5.000E+00	7.456E-06	5.572E+01

% Total harmonic distortion: 1.966E+00

GDF: (from Table A-5)

Freq (HZ)	Fourier Comp	Phase (DEG)
1.000E+00	4.947E-01	9.066E+00
2.000E+00	1.039E-02	1.133E+02
3.000E+00	3.374E-04	3.589E+01
4.000E+00	5.062E-06	1.376E+02
5.000E+00	2.383E-03	5.904E+01

Freq	Initial F_y	Final Voltage (x)	Final F_y
1.000E+00	-5.000E-01 - j5.000E-01	4.885E-01 + j7.795E-02	-6.917E-01 + j5.901E-01
2.000E+00	-5.000E-03 - j5.000E-03	-4.314E-03 + j1.004E-02	1.074E-01 + j2.009E-02
3.000E+00	-5.000E-03 - j5.000E-03	2.734E-04 - j1.978E-04	2.286E-03 - j4.419E-03
4.000E+00	-5.000E-03 - j5.000E-03	-3.739E-06 + j3.413E-06	7.681E-05 + j6.538E-05
5.000E+00	-5.000E-03 - j5.000E-03	1.226E-07 + j2.044E-07	4.818E-06 - j3.344E-06
Freq	Errors	First Derivative	Second Derivative
1.000E+00	-6.994E-06 - j1.291E-05	5.081E-02 - j7.735E-02	1.859E-02 + j2.921E-02
2.000E+00	-7.736E-06 + j1.136E-05	8.805E-04 + j6.416E-04	-1.642E-04 + j1.446E-04
3.000E+00	-8.151E-07 - j6.009E-07	1.597E-05 - j1.630E-05	1.860E-06 + j2.463E-06
4.000E+00	-1.013E-08 + j1.048E-07	1.516E-07 + j2.088E-07	-2.288E-08 + j1.294E-08
5.000E+00	-4.138E-09 + j3.970E-09	8.767E-09 - j4.242E-09	2.810E-10 + j7.447E-10

Table A-5: Small even harmonic distortion with u = 0.5V.

SPECIFICATIONS FOR TABLE A-6

Circuit:	See Figure 4-1
Nonlinearity:	$F(x)^{1/3}$
Voltage Source(u):	$3.0\cos(2\pi)t$
Capacitance(C):	0.1F
Initial λ:	1.000E+00 + j0.000E+00
Final λ:	3.319E+00 + j5.960E-01
Number of Iterations:	27(Converging very slowly)

COMPARISON OF SPICE TRANSIENT ANALYSIS AND THE GDF OUTPUT VOLTAGES

SPICE:

Freq (HZ)	Fourier Comp	Phase (DEG)
1.000E+00	7.597E-01	7.300E+01
2.000E+00	1.129E-05	9.000E+01
3.000E+00	8.007E-02	8.028E+00
4.000E+00	1.129E-05	9.000E+01
5.000E+00	2.489E-02	1.660E+02

% Total harmonic distortion: 1.117E+01

GDF: (from Table A-6)

Freq (HZ)	Fourier Comp	Phase (DEG)
1.000E+00	7.749E-01	7.699E+01
2.000E+00	1.746E-08	2.435E+01
3.000E+00	6.802E-02	1.340E+02
4.000E+00	1.297E-09	-1.412E+02
5.000E+00	2.053E-02	8.856E+01

Freq	Initial F_y	Final Voltage (x)	Final F_y
1.000E+00	-5.000E-01 - j5.000E-01	1.744E-01 + j7.550E-01	1.503E-01 - j1.583E+00
2.000E+00	-5.000E-03 - j5.000E-03	1.591E-08 + j7.201E-09	-1.401E-07 - j6.021E-08
3.000E+00	-5.000E-03 - j5.000E-03	-4.728E-02 + j4.890E-02	3.690E-01 - j1.612E-02
4.000E+00	-5.000E-03 - j5.000E-03	-1.011E-09 - j8.123E-10	7.907E-08 - j1.903E-08
5.000E+00	-5.000E-03 - j5.000E-03	5.168E-04 + j2.052E-02	1.186E-01 - j4.744E-02
Freq	Errors	First Derivative	Second Derivative
1.000E+00	4.034E-03 - j2.637E-03	8.495E-02 + j1.498E-01	-5.518E-02 - j5.311E-02
2.000E+00	1.423E-08 - j1.095E-08	3.461E-09 - j3.858E-10	-1.108E-09 + j8.369E-10
3.000E+00	7.611E-04 - j4.414E-03	-4.805E-04 + j1.177E-02	-2.587E-11 - j5.065E-11
4.000E+00	-5.345E-09 + j1.089E-08	-1.901E-10 + j3.744E-11	2.799E-11 - j5.065E-11
5.000E+00	-4.143E-03 - j4.234E-03	2.244E-03 + j1.424E-03	-6.306E-04 + j2.761E-04

Table A-6: Large odd harmonic distortion with u = 3.0V.

SPECIFICATIONS FOR TABLE A-7

Circuit:	See Figure 4-1
Nonlinearity:	$F(x)^{1/3}$
Voltage Source(u):	$3.0\cos(2\pi)t$
Capacitance(C):	0.1F
Initial λ:	1.000E+00 + j0.000E+00
Final λ:	3.325E+00 + j5.932E-01
Number of Iterations:	18(Converging very slowly)

COMPARISON OF SPICE TRANSIENT ANALYSIS AND THE GDF OUTPUT VOLTAGES

SPICE:

Freq (HZ)	Fourier Comp	Phase (DEG)
1.000E+00	7.597E-01	7.300E+01
2.000E+00	1.129E-05	9.000E+01
3.000E+00	8.007E-02	8.028E+00

% Total harmonic distortion: 1.117E+01

GDF: (from Table A-7)

Freq (HZ)	Fourier Comp	Phase (DEG)
1.000E+00	7.726E-01	7.712E+01
2.000E+00	1.153E-06	4.382E+01
3.000E+00	6.821E-02	1.367E+02

Freq	Initial F_y	Final Voltage (x)	Final F_y
1.000E+00	-5.000E-01 - j5.000E-01	1.772E-01 + j7.532E-01	1.536E-01 - j1.588E+00
2.000E+00	-5.000E-03 - j5.000E-03	8.323E-07 + j7.986E-07	-1.722E-06 - j2.843E-06
3.000E+00	-5.000E-03 - j5.000E-03	-4.961E-02 + j4.682E-02	3.870E-01 - j2.086E-02
Freq	Errors	First Derivative	Second Derivative
1.000E+00	-4.785E-05 + j3.738E-05	8.348E-02 + j1.506E-01	-5.397E-02 - j5.443E-02
2.000E+00	-2.491E-07 - j4.708E-07	2.250E-07 + j5.760E-08	-9.027E-08 + j2.434E-08
3.000E+00	-1.345E-03 + j1.081E-04	-1.345E-03 + j1.196E-02	-2.365E-03 - j3.539E-03

Table A-7: The use of only 3 harmonics in the large odd case.

SPECIFICATIONS FOR TABLE A-8

Circuit:	**See Figure 4-1**
Nonlinearity:	**$F(x)^{1/3}$**
Voltage Source(u):	**$3.0\cos(2\pi)t$**
Capacitance(C):	**0.1F**
Initial λ:	**1.000E+00 + j0.000E+00**
Final λ:	**3.346E+00 + j4.616E-01**
Number of Iterations:	**16**

COMPARISON OF SPICE TRANSIENT ANALYSIS AND THE GDF OUTPUT VOLTAGES

SPICE:

Freq (HZ)	Fourier Comp	Phase (DEG)
1.000E+00	7.597E-01	7.300E+01

GDF: (from Table A-8)

Freq (HZ)	Fourier Comp	Phase (DEG)
1.000E+00	7.639E-01	7.526E+01

Freq	Initial F_y	Final Voltage (x)	Final F_y
1.000E+00	-5.000E-01 - j5.000E-01	1.944E-01 + j7.387E-01	-3.967E-01 - j1.537E+00
Freq	Errors	First Derivative	Second Derivative
1.000E+00	-7.330E-05 - j9.829E-05	8.219E-02 + j1.494E-01	-5.181E-02 - j5.575E-02

Table A-8: The use of only the fundamental in the large odd case.

SPECIFICATIONS FOR TABLE A-9

Circuit:	See Figure 4-1
Nonlinearity:	$F(x)^2$
Voltage Source(u):	$0.6\cos(2\pi)t$
Capacitance(C):	0.1F
Initial λ:	1.000E+00 + j0.000E+00
Final λ:	3.387E+00 + j1.338E+00
Number of Iterations:	23

COMPARISON OF SPICE TRANSIENT ANALYSIS AND THE GDF OUTPUT VOLTAGES

SPICE:

Freq (HZ)	Fourier Comp	Phase (DEG)
1.000E+00	3.513E-01	5.187E+01
2.000E+00	3.593E-02	1.364E+02
3.000E+00	6.510E-03	-1.484E+02
4.000E+00	1.103E-03	-7.573E+01
5.000E+00	1.925E-04	1.106E+00

% Total harmonic distortion: 1.141E+01

GDF: (from Table A-9)

Freq (HZ)	Fourier Comp	Phase (DEG)
1.000E+00	3.202E-01	5.871E+01
2.000E+00	1.831E-02	-1.318E+02
3.000E+00	1.251E-03	-1.510E+02
4.000E+00	8.573E-05	-1.712E+02
5.000E+00	5.888E-06	1.684E+02

Freq	Initial F_y	Final Voltage (x)	Final F_y
1.000E+00	-5.000E-01 - j5.000E-01	1.633E-01 + j2.736E-01	-1.913E-01 - j1.150E+00
2.000E+00	-5.000E-03 - j5.000E-03	-1.221E-02 - j1.365E-02	-1.678E-04 + j1.079E-01
3.000E+00	-5.000E-03 - j5.000E-03	-1.904E-03 - j6.072E-04	1.205E-03 + j9.109E-03
4.000E+00	-5.000E-03 - j5.000E-03	-8.473E-05 - j1.307E-05	2.672E-04 + j7.228E-04
5.000E+00	-5.000E-03 - j5.000E-03	-5.786E-06 + j1.181E-06	3.669E-05 + j5.142E-05
Freq	Errors	First Derivative	Second Derivative
1.000E+00	-3.531E-05 - j1.757E-05	5.484E-02 + j3.777E-02	-2.725E-02 - j5.003E-03
2.000E+00	1.803E-05 + j7.435E-07	-3.090E-03 - j3.427E-04	8.588E-04 - j6.136E-04
3.000E+00	1.588E-06 - j6.684E-07	-1.551E-04 + j7.018E-05	9.853E-06 - j4.527E-05
4.000E+00	1.880E-07 - j1.067E-07	-5.850E-06 + j7.510E-06	-8.239E-07 - j1.947E-06
5.000E+00	1.752E-08 - j1.500E-08	-1.182E-07 + j5.340E-07	-8.166E-08 - j6.047E-08

Table A-9: Large even harmonic distortion with u = 0.6V.

SPECIFICATIONS FOR TABLE A-10

Circuit:	See Figure 4-1
Nonlinearity:	$F(x)^{1/3}$
Voltage Source(u):	$3.0\cos(2\pi)t$
Capacitance(C):	0.1F
Initial λ:	1.000E+00 + j0.000E+00
Final λ:	1.845E+00 + j2.217E-01
Number of Iterations:	15
Weights:	$(1, 0, 0, 0, 0)^T$

COMPARISON OF SPICE TRANSIENT ANALYSIS AND THE GDF OUTPUT VOLTAGES

SPICE:

Freq (HZ)	Fourier Comp	Phase (DEG)
1.000E+00	7.597E-01	7.300E+01
2.000E+00	1.129E-05	9.000E+01
3.000E+00	8.007E-02	8.028E+00
4.000E+00	1.129E-05	9.000E+01
5.000E+00	2.489E-02	1.660E+02

% Total harmonic distortion: 1.117E+01

GDF: (from Table A-10)

Freq (HZ)	Fourier Comp	Phase (DEG)
1.000E+00	7.772E-01	7.722E+01
2.000E+00	3.372E-08	1.389E+02
3.000E+00	8.944E-02	1.365E+02
4.000E+00	1.492E-08	-3.781E+01
5.000E+00	2.680E-02	9.580E+01

Freq	Initial F_y	Final Voltage (x)	Final F_y
1.000E+00	-5.000E-01 - j5.000E-01	1.719E-01 + j7.580E-01	1.503E-01 - j1.552E-01
2.000E+00	-5.000E-03 - j5.000E-03	-2.542E-08 + j2.216E-08	-2.693E-08 + j1.224E-08
3.000E+00	-5.000E-03 - j5.000E-03	-6.489E-02 + j6.156E-02	3.413E-01 - j9.239E-03
4.000E+00	-5.000E-03 - j5.000E-03	1.179E-08 - j9.149E-09	-1.487E-08 + j1.569E-08
5.000E+00	-5.000E-03 - j5.000E-03	-2.710E-03 + j2.666E-02	1.211E-01 - j6.422E-02
Freq	Errors	First Derivative	Second Derivative
1.000E+00	9.772E-07 - j2.094E-06	1.285E-01 + j2.280E-01	-1.269E-01 - j1.224E-01
2.000E+00	0.000E+00 + j0.000E+00	0.000E+00 + j0.000E+00	0.000E+00 + j0.000E+00
3.000E+00	0.000E+00 + j0.000E+00	0.000E+00 + j0.000E+00	0.000E+00 + j0.000E+00
4.000E+00	0.000E+00 + j0.000E+00	0.000E+00 + j0.000E+00	0.000E+00 + j0.000E+00
5.000E+00	0.000E+00 + j0.000E+00	0.000E+00 + j0.000E+00	0.000E+00 + j0.000E+00

Table A-10: Large odd harmonic distortion with weight = $(1, 0, 0, 0, 0)^T$.

SPECIFICATIONS FOR TABLE A-11

Circuit:	**See Figure 4-1**
Nonlinearity:	**$F(x)^{1/3}$**
Voltage Source(u):	**$3.0\cos(2\pi)t$**
Capacitance(C):	**0.1F**
Initial λ:	**1.000E+00 + j0.000E+00**
Final λ:	**1.841E+00 + j2.216E-01**
Number of Iterations:	**17**
Weights:	**$(1, 0, 1, 0, 0)^T$**

COMPARISON OF SPICE TRANSIENT ANALYSIS AND THE GDF OUTPUT VOLTAGES

SPICE:

Freq (HZ)	Fourier Comp	Phase (DEG)
1.000E+00	7.597E-01	7.300E+01
2.000E+00	1.129E-05	9.000E+01
3.000E+00	8.007E-02	8.028E+00
4.000E+00	1.129E-05	9.000E+01
5.000E+00	2.489E-02	1.660E+02

% Total harmonic distortion: 1.117E+01

GDF: (from Table A-11)

Freq (HZ)	Fourier Comp	Phase (DEG)
1.000E+00	7.771E-01	7.722E+01
2.000E+00	3.487E-08	8.506E+01
3.000E+00	8.940E-02	1.366E+02
4.000E+00	1.137E-08	8.185E+01
5.000E+00	2.679E-02	9.589E+01

Freq	Initial F_y	Final Voltage (x)	Final F_y
1.000E+00	-5.000E-01 - j5.000E-01	1.719E-01 + j7.579E-01	1.557E-01 - j4.141E-01
2.000E+00	-5.000E-03 - j5.000E-03	3.005E-09 + j3.474E-08	-8.661E-08 - j6,283E-08
3.000E+00	-5.000E-03 - j5.000E-03	-6.501E-02 + j6.137E-02	3.413E-01 - j8.542E-03
4.000E+00	-5.000E-03 - j5.000E-03	1.613E-09 + j1.126E-08	-2.692E-08 - j1.808E-08
5.000E+00	-5.000E-03 - j5.000E-03	-2.751E-03 + j2.665E-02	1.212E-01 - j6.406E-02
Freq	Errors	First Derivative	Second Derivative
1.000E+00	-3.375E-06 - j4.190E-05	1.288E-01 + j2.283E-01	-1.273E-01 - j1.226E-01
2.000E+00	0.000E+00 + j0.000E+00	0.000E+00 + j0.000E+00	0.000E+00 + j0.000E+00
3.000E+00	-5.349E-05 + j1.630E-05	-1.936E-03 + j2.334E-02	-7.415E-03 - j9.782E-03
4.000E+00	0.000E+00 + j0.000E+00	0.000E+00 + j0.000E+00	0.000E+00 + j0.000E+00
5.000E+00	0.000E+00 + j0.000E+00	0.000E+00 + j0.000E+00	0.000E+00 + j0.000E+00

Table A-11: Large odd harmonic distortion with weight = $(1, 0, 1, 0, 0)^T$.

SPECIFICATIONS FOR TABLE A-12

Circuit:	**See Figure 4-1**
Nonlinearity:	**F(x)** $^{1/3}$
Voltage Source(u):	**3.0cos(2π)t**
Capacitance(C):	**0.1F**
Initial λ:	**1.000E+00 + j0.000E+00**
Final λ:	**1.846E+00 + j2.216E-01**
Number of Iterations:	**13**
Weights:	**Normalized Output**

COMPARISON OF SPICE TRANSIENT ANALYSIS AND THE GDF OUTPUT VOLTAGES

SPICE:

Freq (HZ)	Fourier Comp	Phase (DEG)
1.000E+00	7.597E-01	7.300E+01
2.000E+00	1.129E-05	9.000E+01
3.000E+00	8.007E-02	8.028E+00
4.000E+00	1.129E-05	9.000E+01
5.000E+00	2.489E-02	1.660E+02

% Total harmonic distortion: 1.117E+01

GDF: (from Table A-12)

Freq (HZ)	Fourier Comp	Phase (DEG)
1.000E+00	7.769E-01	7.723E+01
2.000E+00	7.020E-08	8.801E+01
3.000E+00	8.976E-02	1.365E+02
4.000E+00	1.373E-08	1.686E+02
5.000E+00	2.684E-02	9.573E+01

Freq	Initial F_y	Final Voltage (x)	Final F_y
1.000E+00	-5.000E-01 - j5.000E-01	1.717E-01 + j7.577E-01	1.553E-01 - j4.175E-01
2.000E+00	-5.000E-03 - j5.000E-03	-2.442E-09 + j7.016E-08	-3.342E-08 - j1.022E-07
3.000E+00	-5.000E-03 - j5.000E-03	-6.515E-02 + j6.175E-02	3.421E-01 - j9.810E-03
4.000E+00	-5.000E-03 - j5.000E-03	-1.346E-08 + j2.721E-09	1.335E-08 + j4.630E-08
5.000E+00	-5.000E-03 - j5.000E-03	-2.678E-03 + j2.671E-02	1.210E-01 - j6.445E-02
Freq	Errors	First Derivative	Second Derivative
1.000E+00	3.392E-05 + j4.361E-05	1.275E-01 + j2.263E-01	-1.249E-01 - j1.206E-01
2.000E+00	1.975E-15 - j4.383E-15	1.030E-15 + j1.596E-15	-9.217E-23 - j4.557E-23
3.000E+00	2.165E-05 - j1.253E-05	-2.197E-04 + j2.685E-03	-9.772E-05 - j1.288E-04
4.000E+00	0.000E+00 + j0.000E+00	0.000E+00 + j0.000E+00	0.000E+00 + j0.000E+00
5.000E+00	0.000E+00 + j0.000E+00	0.000E+00 + j0.000E+00	0.000E+00 + j0.000E+00

Table A-12: Large odd harmonic distortion with normalized weights.

SPECIFICATIONS FOR TABLE A-13

Circuit:	**See Figure 4-1**
Nonlinearity:	**$F(x)^2$**
Voltage Source(u):	**$0.6\cos(2\pi)t$**
Capacitance(C):	**0.1F**
Initial λ:	**1.000E+00 + j0.000E+00**
Final λ:	**1.878E+00 + j4.228E-01**
Number of Iterations:	**16**
Weights:	**Normalized Output**

COMPARISON OF SPICE TRANSIENT ANALYSIS AND THE GDF OUTPUT VOLTAGES

SPICE:

Freq (HZ)	Fourier Comp	Phase (DEG)
1.000E+00	3.513E-01	5.187E+01
2.000E+00	3.593E-02	1.364E+02
3.000E+00	6.510E-03	-1.484E+02
4.000E+00	1.103E-03	-7.573E+01
5.000E+00	1.925E-04	1.106E+00

% Total harmonic distortion: 1.141E+01

GDF: (from Table A-13)

Freq (HZ)	Fourier Comp	Phase (DEG)
1.000E+00	3.193E-01	5.911E+01
2.000E+00	2.579E-02	-1.218E+02
3.000E+00	2.837E-03	-1.325E+02
4.000E+00	3.204E-04	-1.534E+02
5.000E+00	1.489E-05	-1.524E+02

Freq	Initial F_y	Final Voltage (x)	Final F_y
1.000E+00	-5.000E-01 - j5.000E-01	1.639E-01 + j2.740E-01	-1.835E-01 - j5.840E-01
2.000E+00	-5.000E-03 - j5.000E-03	-1.359E-02 - j2.192E-02	-6.975E-03 + j9.162E-02
3.000E+00	-5.000E-03 - j5.000E-03	-1.918E-03 - j2.090E-03	-1.061E-03 + j1.205E-02
4.000E+00	-5.000E-03 - j5.000E-03	-2.622E-04 - j1.783E-04	1.603E-05 + j1.612E-03
5.000E+00	-5.000E-03 - j5.000E-03	-1.320E-05 - j6.895E-06	2.128E-05 + j8.896E-05
Freq	Errors	First Derivative	Second Derivative
1.000E+00	-1.576E-06 + j3.661E-05	8.064E-02 + j6.546E-02	-6.389E-02 - j2.202E-02
2.000E+00	6.067E-07 + j1.107E-07	-5.399E-04 - j2.187E-04	2.553E-05 - j6.409E-06
3.000E+00	3.032E-09 + j2.397E-08	-5.885E-06 + j1.370E-08	1.643E-08 - j1.807E-08
4.000E+00	0.000E+00 + j0.000E+00	0.000E+00 + j0.000E+00	0.000E+00 + j0.000E+00
5.000E+00	0.000E+00 + j0.000E+00	0.000E+00 + j0.000E+00	0.000E+00 + j0.000E+00

Table A-13: Large even harmonic distortion with normalized output weights.

SPECIFICATIONS FOR TABLE A-14

Circuit:	**See Figure 4-1**
Nonlinearity:	**$F(x)^{1/3}$**
Voltage Source(u):	**$3.0\cos(2\pi)t$**
Capacitance(C):	**1.0F**
Initial λ:	**1.000E+00 + j0.000E+00**
Final λ:	**7.817E-01 - j1.452E-01**
Number of Iterations:	**4**
Weights:	**Normalized Output**

COMPARISON OF SPICE TRANSIENT ANALYSIS AND THE GDF OUTPUT VOLTAGES

SPICE:

Freq (HZ)	Fourier Comp	Phase (DEG)
1.000E+00	2.908E+00	1.401E+01
2.000E+00	3.056E-05	9.079E+01
3.000E+00	1.741E-02	1.367E+02
4.000E+00	3.057E-05	9.042E+01
5.000E+00	5.160E-03	1.641E+02

% Total harmonic distortion: 6.307E-01

GDF: (from Table A-14)

Freq (HZ)	Fourier Comp	Phase (DEG)
1.000E+00	2.910E+00	1.402E+01
2.000E+00	2.153E-07	3.997E+01
3.000E+00	1.779E-02	-4.302E+01
4.000E+00	9.001E-09	-5.873E+01
5.000E+00	5.361E-03	1.644E+02

Freq	Initial F_y	Final Voltage (x)	Final F_y
1.000E+00	-5.000E-01 - j5.000E-01	2.823E+00 + j7.047E-01	-7.048E-01 + j2.672E-01
2.000E+00	-5.000E-03 - j5.000E-03	1.650E-07 + j1.383E-07	-2.296E-07 + j6.142E-08
3.000E+00	-5.000E-03 - j5.000E-03	1.301E-02 - j1.214E-02	-2.468E-01 - j2.180E-01
4.000E+00	-5.000E-03 - j5.000E-03	4.672E-09 - j7.694E-09	5.799E-08 - j5.228E-08
5.000E+00	-5.000E-03 - j5.000E-03	-5.162E-03 + j1.445E-03	5.345E-02 + j1.560E-01
Freq	Errors	First Derivative	Second Derivative
1.000E+00	3.075E-05 - j1.056E-05	2.290E-01 - j3.935E-01	9.831E-02 + j1.302E-01
2.000E+00	-1.238E-14 - j1.164E-14	9.580E-16 - j8.588E-16	8.461E-24 + j1.278E-23
3.000E+00	3.707E-08 + j1.735E-08	-3.582E-06 - j4.667E-06	3.299E-09 - j2.060E-09
4.000E+00	0.000E+00 + j0.000E+00	0.000E+00 + j0.000E+00	0.000E+00 + j0.000E+00
5.000E+00	0.000E+00 + j0.000E+00	0.000E+00 + j0.000E+00	0.000E+00 + j0.000E+00

Table A-14: Small odd harmonic distortion with normalized output weights.

SPECIFICATIONS FOR TABLE A-15

Circuit:	See Figure 4-1
Nonlinearity:	$F(x)^2$
Voltage Source(u):	$0.5\cos(2\pi)t$
Capacitance(C):	1.0F
Initial λ:	1.000E+00 + j0.000E+00
Final λ:	1.092E-00 + j8.171E-01
Number of Iterations:	7
Weights:	Normalized Output

COMPARISON OF SPICE TRANSIENT ANALYSIS AND THE GDF OUTPUT VOLTAGES

SPICE:

Freq (HZ)	Fourier Comp	Phase (DEG)
1.000E+00	4.959E-01	6.454E+00
2.000E+00	9.745E-03	1.616E+01
3.000E+00	2.623E-04	2.536E+01
4.000E+00	1.475E-05	4.243E+01
5.000E+00	7.456E-06	5.572E+01

% Total harmonic distortion: 1.966E+00

GDF: (from Table A-15)

Freq (HZ)	Fourier Comp	Phase (DEG)
1.000E+00	4.948E-01	9.056E+00
2.000E+00	1.039E-02	1.130E+02
3.000E+00	2.981E-04	3.524E+01
4.000E+00	4.196E-06	1.370E+02
5.000E+00	1.114E-07	6.066E+01

Freq	Initial F_y	Final Voltage (x)	Final F_y
1.000E+00	-5.000E-01 - j5.000E-01	4.866E-01 + j7.788E-02	-5.958E-01 + j3.092E-01
2.000E+00	-5.000E-03 - j5.000E-03	-4.058E-03 + j9.560E-03	1.131E-01 + j2.436E-02
3.000E+00	-5.000E-03 - j5.000E-03	2.435E-04 + j1.720E-04	2.321E-03 - j4.434E-03
4.000E+00	-5.000E-03 - j5.000E-03	-3.066E-06 + j2.864E-06	6.910E-05 + j5.858E-05
5.000E+00	-5.000E-03 - j5.000E-03	5.465E-08 + j9.708E-08	2.492E-06 - j1.690E-06
Freq	Errors	First Derivative	Second Derivative
1.000E+00	3.227E-06 - j1.588E-05	4.226E-02 - j7.320E-02	1.820E-02 + j2.242E-02
2.000E+00	-2.357E-08 + j1.159E-07	1.627E-05 + j1.090E-05	-5.192E-08 + j5.252E-08
3.000E+00	-3.901E-10 + j2.698E-10	7.342E-09 - j8.008E-09	5.113E-13 + j6.047E-13
4.000E+00	0.000E+00 + j0.000E+00	0.000E+00 + j0.000E+00	0.000E+00 + j0.000E+00
5.000E+00	0.000E+00 + j0.000E+00	0.000E+00 + j0.000E+00	0.000E+00 + j0.000E+00

Table A-15: Small even harmonic distortion with normalized output weights.

Vita

Ibarra C. Jaculbe III. received his Bachelor of Science in Electrical Engineering degree from Silliman University in Dumaguete City, Philippines in 1986, and passed the national electrical engineering licensure examinations of the Philippines in the same year. He worked as an instructor at Silliman University from 1987 to 1989, and during that same period, he was a part-time designer and supervisor of electrical works in various construction projects in Dumaguete city. He came Lehigh University in the fall of 1989, and is currently pursuing his Master of Science degree in Electrical Engineering.